Fabian Wiedemaier, BSc

Rhenium(V) catalyzed nitrate reduction

MASTER THESIS

to achieve the university degree of

Master of Science

Master degree program: Chemistry

submitted to

Graz University of Technology

Supervisor

Assoz.Prof. Mag.rer.nat Jörg Schachner, PhD

Institute of Chemistry, University of Graz

Graz, June 2019

AFFIDAVIT

I declare that I have authored this thesis independently, that I have not used other than the declared sources/resources, and that I have explicitly indicated all material which has been quoted either literally or by content from the sources used. The text document uploaded to TUGRAZonline is identical to the present master thesis.

Date	Signature

Acknowledgment

I would like to express my deepest gratitude to my supervisor Assoz. Prof. Dr. Jörg Schachner for letting me be a part of this challenging and exciting project. I really appreciated the frequent and sometimes long-lasting discussions, while at the same time I had the freedom to develop and to implement my own ideas.

Thanks should also go to Univ.-Prof. Dr. Nadia C. Mösch-Zanetti for giving me the opportunity to work in her group.

Special thanks to ao. Univ.-Prof. Dr. Ferdinand Belaj for analyzing my single-crystals and solving their molecular structures, no matter if organic or inorganic.

Despite not being present in this work, I would like to thank Univ. Prof. Dr. Adrian D. Boese for supporting and supervising my theoretical investigations on this project during my bachelor thesis and later on.

I gratefully acknowledge the assistance of the team around Doris Eibinger. Doing research in chemistry would hardly be possible without a well working laboratory. Especially our apprentice Lara was a big help by taking care of the glassware and by keeping our small laboratory well supplied.

I also had great pleasure of working with all the other people in the group, especially Carina, Madeleine, my follow master-student Karin, Antoine, Hristo, Riccardo and Simon.

Special thanks also to my esteemed friends and fellow students for accompanying me for the last years.

I cannot begin to express my thanks to my family, who supported me throughout the last years in one way or another, especially my parents for their unconditional and unquestioned support throughout the last decade. Such a freedom to shape one’s own life is a priceless gift.

Abstract

The oxorhenium(V) complex **2** was investigated concerning its capability of catalytically reducing nitrate. This nitrate degradation is thought to occur via an oxygen atom transfer (OAT) based catalytic cycle where the first OAT step transfers an oxygen atom from the nitrate to the catalyst, resulting in the formation of nitrite and a dioxorhenium(VII) cation **3**. This dioxorhenium(VII) subsequently is reduced again by an OAT to an organic sulfide, which acts as the terminal oxygen acceptor. This sulfoxidation regenerates **2** and closes the catalytic cycle of nitrate reduction. Different kinetic experiments were performed which confirm this first reduction of the nitrate to occur via the proposed OAT mechanisms. They also gave further insight in the behavior of the catalytic system and identified the OAT from the nitrate to the catalyst as the turnover-limiting step with an activation barrier of 65 ± 2 kJ mol^{-1}. The further reaction of the oxorhenium(V) catalyst with the nitrite generated in the first reduction turns out to proceed similar to a common pathway known in biological denitrification. In contrast to the first reduction, the oxygen transfer from nitrite to the catalyst is not accompanied by a two-electron oxidation, but rather by a one-electron oxidation. The resulting neutral dioxorhenium(VI) complex **3'** was isolated from a catalytic experiment and later on independently synthesized and fully characterized. Further studies showed that this complex is not active concerning sulfoxidation. As a consequence the active oxorhenium(V) catalyst cannot be regenerated and the catalytic cycle cannot be closed. This dioxorhenium(VI) complex **3'** is therefore thought to be catalytically inactive in nitrate degradation. The formation of **3'** is accompanied by the generation of nitric oxide, NO. This small molecule is itself not reactive in OAT reactions. When molecular oxygen is present it is oxidized to NO_2 which than is a very potent oxygen donor that is able to perform both sulfoxidation or OAT to the oxorhenium(V) complex **2**, which results in the formation of dioxorhenium(VII) cation **3**, which is also capable of sulfoxidation. Under aerobic conditions nitric oxide therefore catalyzes the sulfoxidation with molecular oxygen.

Table of Contents

List of Figures

List of Tables

1 Introduction

1.1 Oxygen atom transfer (OAT)

Oxygen atom transfer (OAT) reactions are a well-known type of chemical reaction that follow a reaction mechanism as shown in Figure 1. In the general case, an oxygen atom is transferred from a substrate XO to an oxygen-atom-acceptor Y resulting in the formation of YO. At this point it is important to note that formally just an oxygen atom including its 6 valence-electrons is transferred and not an oxide O^{2-} with a complete electron octet and two negative charges. In metal catalyzed OAT reactions, the oxygen atom is initially transferred to the metal catalyst. This OAT results on an oxo-metal complex, where the oxidation number of the metal is increased by two. Consequently a trivial requirement for this OAT to happen is the possibility of the metal to exist in this two oxidation states z and z+2. Also the resulting oxo-metal complex has to stable at least on a time scale that allows the acceptor Y to abstract the oxygen atom.[1]

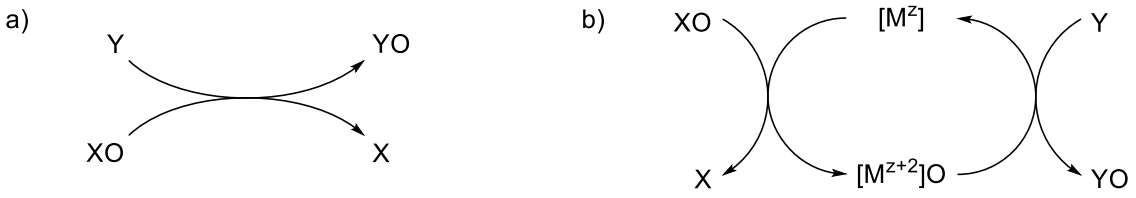

Figure 1 a) General OAT reaction scheme, where an oxygen atom is transferred from a substrate XO to an acceptor Y b) Metal catalyzed OAT, where the oxygen atom is transferred from a substrate XO via the metal catalyst [M] to the substrate Y; z denotes the oxidation number of the metal center

1.2 Perchlorate reduction

Although the electrochemical half-reaction $ClO_4^- + 2\ H^+ + 2\ e^- \rightarrow ClO_3^- + H_2O$ is exergonic, as indicated by its rather high standard reduction potential of $E^o = 1.23$ V (vs SHE)[2], the activation of perchlorate by a transition metal catalyzed OAT mechanism presents itself as a challenge because of the non-labile character of the perchlorate anion.[1,3,4] Nevertheless, biology has found a way to overcome this obstacle, and there are several organisms known which even can live on (per)chlorate as terminal electron sink.[5–7] Those biological systems are thought to consist of two distinct enzyme systems. Initially the (per)chlorate reductase

reduces the oxoanions in two consecutive steps to the chlorite anion. The chlorite dismutase then catalyzes the disproportionation of the chlorite into chloride and molecular oxygen (Figure 2).[5,6,8]

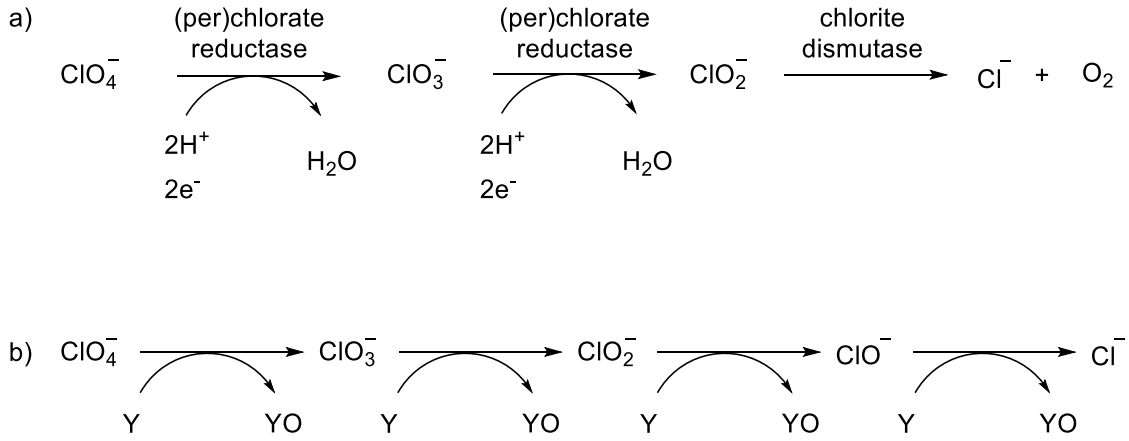

Figure 2. a) Proposed degradation pathway of perchlorate in microorganisms[5,6] b) Step by step perchlorate degradation via transition metal catalyzed OAT mechanism, where Y is a general oxygen acceptor

In 1996 Abu-Omar described in his pioneering work the degradation of perchlorate by a rhenium catalyzed OAT mechanism, in which hypophosphorous acid acts as oxygen acceptor. During this catalytic cycle an oxygen atom from the ClO_x^- anion is transferred to a methylrhenium dioxide. The hypophosphorous acid subsequently reduces the formed methylrhenium trioxide to close the catalytic cycle.[9,10] Further developments lead to an oxorhenium(V) based system bearing two phenolate-oxazoline ligands. This system is capable of catalytically reducing perchlorate (Figure 3). Mechanistic studies suggest an OAT mechanism where again the oxo ligands are transferred from the oxoanion, via the catalyst, to a substrate, in this case an organic sulfide. The initial loss of the chloro ligand and its substitution by a solvent molecule results in the formation of a cationic complex, which is thought to be the active intermediate within the catalytic cycle. This cation was also synthesized and characterized as its corresponding triflate salt by adding silver triflate to a solution of the chloro-complex in acetonitrile. The following step in the catalytic cycle is substitution of the coordinated solvent molecule by the oxoanion ClO_x^-, initially the perchlorate. This substitution yields an asymmetric, short-lived, neutral complex in which the rhenium still occupies an oxidation state of V. Subsequently a cationic dioxo-complex is formed,

accompanied by an oxidation of the rhenium center to Re(VII) and the loss of the now reduced oxoanion ClO_{n-1}^-. This is considered to be the turnover-limiting step, which is supported by experimental and also theoretical investigations. As this dark red to brown Re(VII)-dioxo cationic species seems to play a crucial role during catalysis, it is unfortunate that it was not fully characterized so far. Finally, the catalytic cycle is closed by the oxygen-atom-transfer from the dioxo-cation to an organic sulfide and again the coordination of a solvent molecule to give the cationic Re(V) intermediate.[4,11]

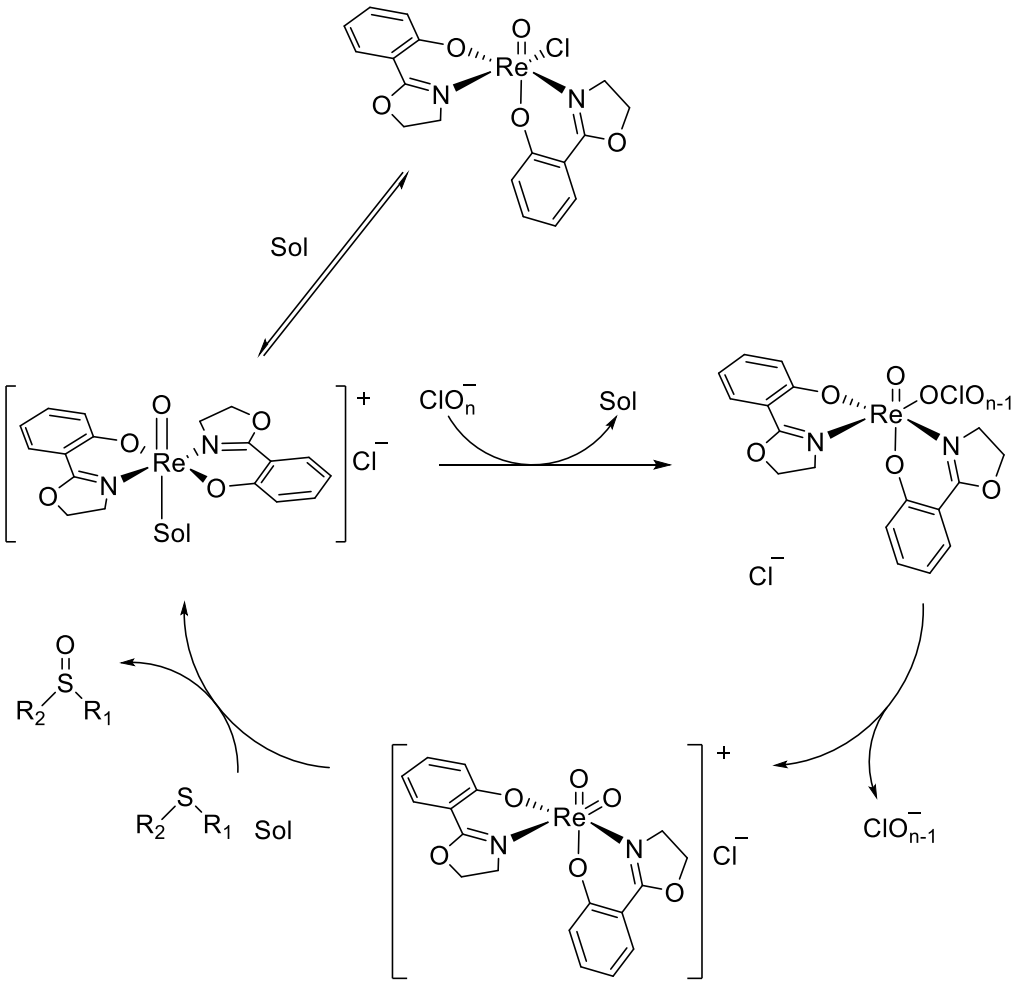

Figure 3 Catalytic cycle of the oxorhenium(V) based perchlorate reduction as suggested by Abu-Omar et al.[4,11]; Sol is a solvent molecule

In contrast to the biological dominant pathway as shown in Figure 2, this OAT based system is thought to fully reduce the perchlorate substrate to chloride without the disproportionation of the chlorite, so no molecular oxygen is formed

and four equivalents of the oxygen-atom-acceptor, the organic sulfide, in terms of perchlorate are consumed during the degradation.

1.3 Nitrate reduction

Nitrogen is among the most abundant elements in the solar system and the main constituent of our atmosphere. Although it is chemically inert in its molecular form, biology and later also human technology managed to make it available as a fundamental biochemical building block of life. Earths nitrogen cycle starts with the fixation of molecular nitrogen from the atmosphere leading to the two most abundant nitrogen-species in biological systems, ammonium and nitrate. Both of them represent the general boundaries for the oxidation states of nitrogen, ammonium (-III), and nitrate (+V). Although the second part of the nitrogen cycle, the denitrification, can also occur from ammonium, the classical cycle proceeds via nitrate. It is worth to note that especially under anaerobic conditions, nitrate can also act as a terminal electron-sink within biological metabolisms.[3,12–14] In contrast to perchlorate, the nitrate anion has an uneven oxidation number. In general this excludes a pure OAT mechanism for the degradation of this oxoanion. Because of the terminal degradation product being molecular nitrogen, at least one single-electron-transfer has to occur throughout the reduction. In biology the denitrification process plays a major role because it closes the nitrogen-cycle. The most common pathway occurring in bacterial denitrification is shown in Figure 4.[12,15–17]

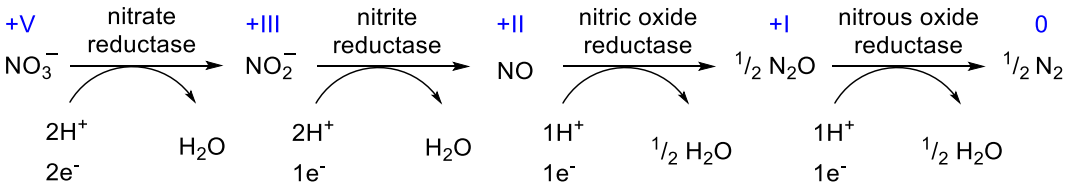

Figure 4 The dominant bacterial denitrification pathway, with oxidation states of nitrogen shown in blue[12,15–17]

Initially the nitrate is reduced by a nitrate reductase to give the nitrite anion. These two-electron reducing systems are in general metalloenzymes that contain transition-metals[15], often molybdenum.[18–21] Especially in these molybdenum

containing enzymes nitrate reduction was previously described to occur via an OAT mechanism, where one of the nitrate oxygens is transferred to an oxomolybdenum(IV) moiety to give a dioxomolybdenum(VI) species. This oxygen atom is subsequently protonated twice and the molybdenum center is reduced by two electrons. The release of a water molecule then closes the catalytic cycle.[21] This first reduction is comparable with the initial reduction of perchlorate (Figure 2), where also a two-electron reduction is accompanied by an oxygen loss. Also in case of (per)chlorate reductases molybdenum containing enzymes are known.[8] In contrast to perchlorate reduction, the second step of the denitrification cascade does not occur via a two-electron reduction, but rather a one-electron reduction. Despite this one-electron transfer, also molybdenum based enzymes, which usually catalyze two-electron OAT steps, are reported to reduce nitrite, although iron and cupper based enzymes are considered to play a dominant role.[15,17,22–25] Similar to nitrate reduction, again an oxygen atom from the nitrite is transferred to an oxomolybdenum(IV) metal center, but the release of the nitric oxide results in the formation of a Mo(V) species rather than Mo(VI).[22,24] The subsequent reaction of two nitric oxide molecules resulting in the formation of nitrous oxide, or dinitrogen oxide, is usually catalyzed by cupper and iron based metalloenzymes containing two neighboring metal atoms. In those enzymes each of the two nitric oxide molecules is binding to one of the two neighboring metal atoms. The following release of the nitrous oxide is supposed to result in the formation of a μ-oxo bridge between the neighboring metal atoms, which is accompanied by an oxidation of the metal centers. Protonation of the μ-O atom and the reduction of the metal centers closes the catalytic cycle.[15,26–31] The reduction of nitrous oxide is the final reaction during the denitrification process. Here the reduction is thought to occur at a tetrahedral cluster that consists of a central sulfur atom which is surrounded by four cupper atoms.[16,32]

1.4 General aspects regarding catalytic denitrification

Because of the overall importance of the nitrogen cycle and the broad abundance of nitrogen containing species in all living organisms, the denitrification process is a long established field of research.[12,13,17] Especially the degradation starting

from nitrate is of interest, also because of its still increasing anthropological discharge in the environment, especially via agricultural usage in fertilizers.[33–37] Numerous attempts towards denitrification were made, mainly inspired by the biological nitrogen pathway.[17] A possible pathway for transition-metal catalyzed nitrate degradation is shown in Figure 5.

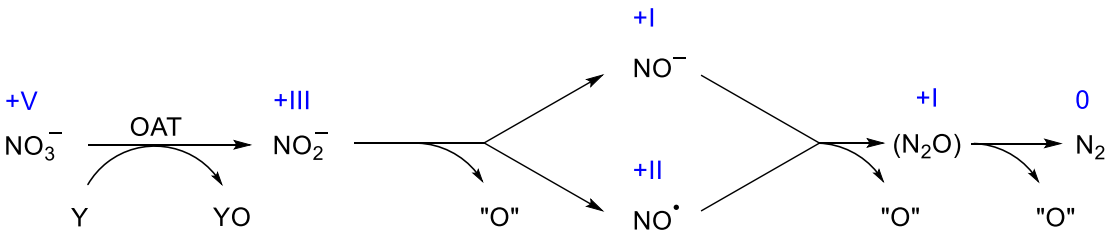

Figure 5 Possible pathway for transition-metal catalyzed nitrate degradation

A possible initial step in catalytic nitrate degradation is the formation of nitrite by a pure OAT mechanism. This would be in analogy to the molybdenum based nitrate reductases, where also an OAT mechanism is suggested (vide supra). The resulting nitrite is a reasonable product because it is itself a stable, common anion which forms stable salts that have a wide range of applications, for example in the chemical and pharmaceutical industry they are used in the production of nitroso-compounds or during diazotization-reactions and of course as food preservative.[3,38] As in the nitrate reductases occurring in biology, also most of the currently known model complexes are based on molybdenum.[39–44] Subsequently also tungsten based systems have been developed.[41,45,46] A common moiety that can be found in most of those systems is the dithiolene motif, mimicking the molybdopterin cofactor.[41,44] Another common feature of some model complexes is the oxo ligand in their initial, reduced form. The addition of nitrate to those models results in the formation of a *cis*-dioxo complex, which is also supposed to occur in the molybdenum based nitrate reductases.[21,39–41] Difficulties arise during the second step in nitrate degradation, the reduction of the nitrite. In principle another OAT-type reaction could occur resulting in the rather unstable nitroxyl-anion NO^-. On the other hand the loss of the oxygen atom at the nitrogen can be accompanied by a one-electron reduction yielding nitric oxide NO, in line with the biological pathway. Because of its positive standard

enthalpy of formation and its unpaired electron, also nitric oxide, or nitrogen monoxide, represents a rather reactive species. When in contact with atmospheric oxygen, it immediately reacts in an exothermic reaction to give nitrogen dioxide NO_2. At high pressure and elevated temperatures the reaction $3\,NO \rightarrow N_2O + NO_2$ occurs.[3,15,47–49] In contrast to nitrate reductase, model chemistry for the nitrite reductase focuses on copper and iron based complexes[15,50–53], although also molybdenum based systems are known.[54] Whatever diatomic fragment has been formed at this point, further transition-metal catalyzed reduction most certainly includes the coordination of an NO fragment towards the metal. Such nitrosyl complexes have been studied as functional models for nitric oxide reductase, where iron[55–57] and copper[58,59] systems are predominant. A common feature of those systems is the formation and release of nitrous oxide N_2O, so no further reduction to molecular nitrogen takes place. Despite the rather complex structure of the nitrous oxide reductase with its cupper sulfur cluster, functional model complexes were developed. They are in general based on a binuclear Cu_2S motif mimicking the cupper sulfur cluster and complete the nitrate degradation by the release of molecular nitrogen.[60–62]

1.5 Objective

This research project intends to investigate the reactivity of an oxorhenium(V) based system, similar to the one used by Abu-Omar during his studies of perchlorate degradation, regarding nitrate degradation. Especially for the first step of the denitrification, the reduction of nitrate to nitrite, this rhenium based system seems promising, as in the biological pathways this step is catalyzed by molybdenum based enzymes, which is diagonally related to rhenium. The essential oxorhenium system as shown in Figure 3 was studied extensively in terms of perchlorate reduction.[4,11,63] In general four types of isomers can be drawn for this oxorhenium system (where the oxo and the chloro ligand are *cis* to each other), which are depicted in Figure 6. So far mainly isomers of type A and B are reported, where the phenolate is *trans* to the oxo ligand. Kinetic studies showed that the so called N,N-*trans* isomer (isomer A in Figure 6) represents the

most catalytically active species, at least regarding perchlorate degradation.[64,65] Most recently successful approaches towards the preparation of the pure N,N-*trans* isomer were published.[64,66,67]

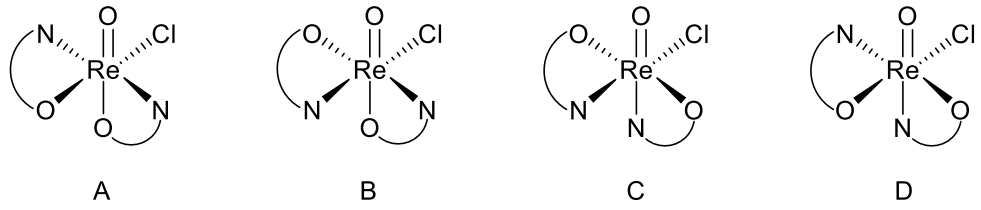

Figure 6 Possible isomers of the studied oxorhenium system; in general only A and B are observed

The system chosen for these studies is complex **2**, published by Schachner in 2019, depicted in Figure 7.[67] In this case the N,N-*trans* selectivity is achieved by the introduction of two methyl-groups at the carbon atom next to the nitrogen in the oxazoline moiety.

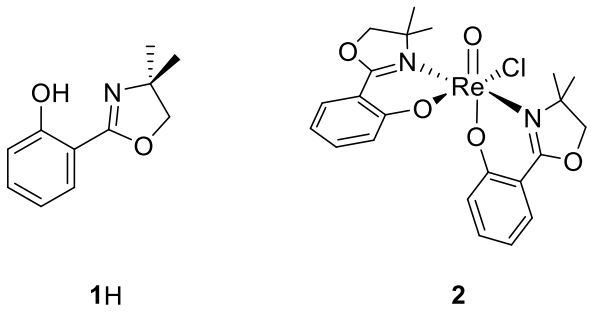

Figure 7 The ligand **1**H and the phenolate-oxazoline based oxorhenium(V) complex **2** introduced by Schachner[67]

In general this complex is an example of a d^2 oxo-complex. Their electronic structure has been extensively studied initiated by the fundamental work of Ballhausen and Gray on the subject of the vanadyl-ion VO^{2+}.[68,69] The d-orbital splitting as depicted in Figure 8 predicts stable d^2 oxo-complexes whose geometry can be described within a C_{4v} point group. Both d-electrons occupy the non-bonding d_{xy}-orbital, whereas the antibonding π-orbitals remain unoccupied and the bond order of the metal-oxo bond remains 3. Because of the occupation of only a non-bonding orbital these d^2 oxo-complexes are rather stable and numerous examples are known.[1] Such oxorhenium(V) systems have been studied regarding their abilities in OAT reactions.[70–73]

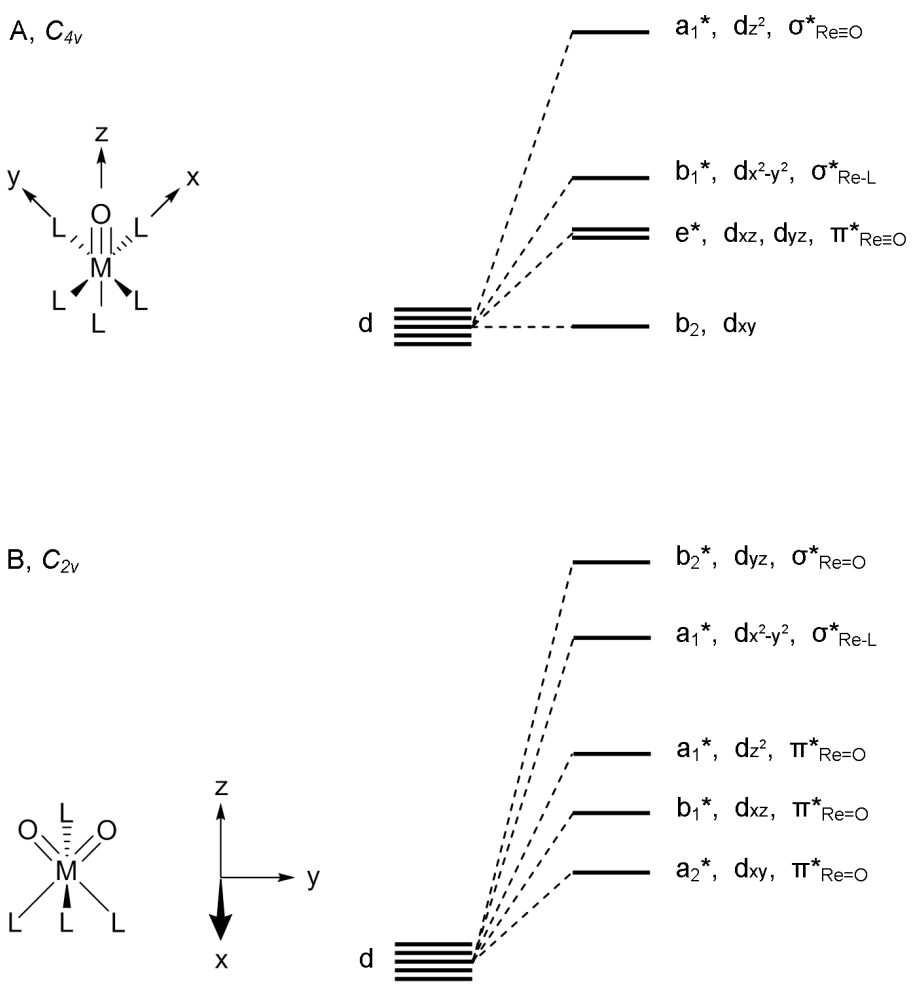

Figure 8 Relevant sections of the MO schemes of A) An oxo-complex within the point group C_{4v} as proposed by Ballhausen and Gray[68,69]; B) A *cis* dioxo-complex within the point group C_{2v}[74,75]

A common conclusion of those investigation is the formation of a *cis*-dioxorhenium(VII) species via the loss of one ligand accompanied by the formation of a more or less square pyramidal intermediate as shown in Figure 9.

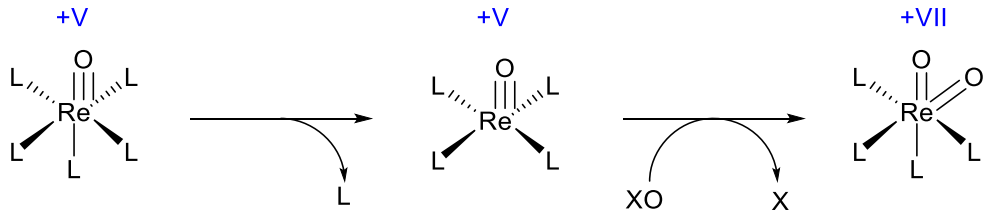

Figure 9 Proposed formation of a dioxorhenium(VII) species as a first step in OAT reactions via the formation of a square pyramidal oxorhenium(V) complex[70–73]

As such square pyramidal complexes possess C_{4v} symmetry, the general electronic situation remains unchanged and the d-orbital scheme in Figure 8 still applies. The subsequent formation of the oxidized dioxo species reduces the symmetry to C_{2v}. Consequently, also the electronic situation changes (Figure 8). The formerly non-bonding d_{xy}-orbital now takes part in the oxo-metal π-bonding. The d^0 configuration of a dioxorhenium(VII) should support this new bonding situation because all of the now antibonding d-orbitals remain unoccupied. Whereas numerous examples of molybdenum d^0 *cis*-dioxo-complexes are known and well characterized,[1] only a few dioxorhenium(VII) compounds are fully characterized so far, and none of them being a cation.[11,71,76]

2 Results and Discussion

2.1 Reactivity regarding Nitrate

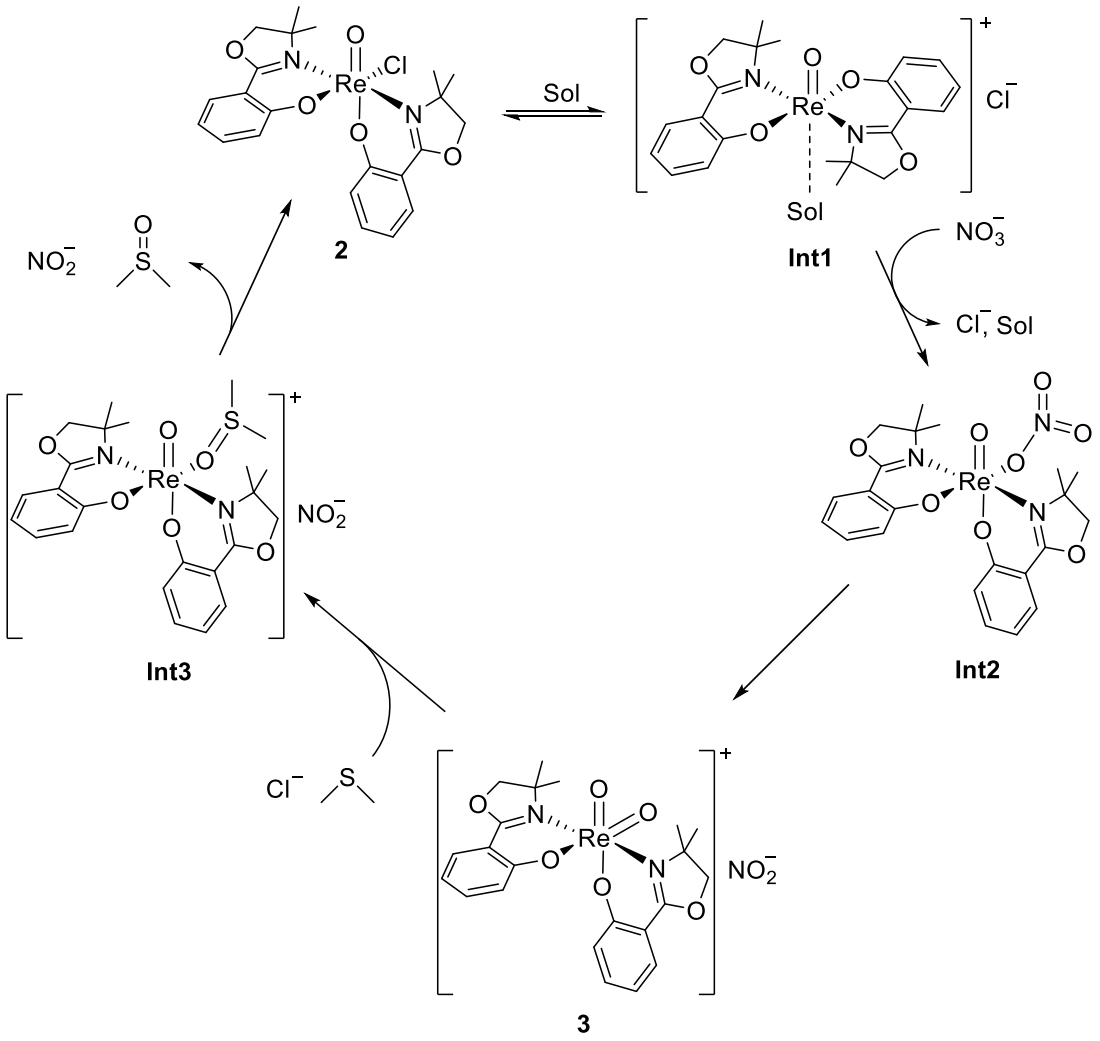

Figure 10 Proposed catalytic cycle for the reduction of nitrate to nitrite catalyzed by **2**; Sol is a solvent molecule

Assuming a similar reactivity with nitrate than with perchlorate (Figure 3), the first reduction of the substrate can be drawn as an OAT reaction, depicted in Figure 10. Also here the initial step is the formation of a symmetric, cationic solvent-adduct **Int1** accompanied by the loss of the chloro ligand. The coordination of the solvent molecule can be assumed *trans* to the oxo ligand, because this preserves the two-fold symmetry that leads to an MO-scheme similar to the one for oxo-complexes as shown in Figure 8. In this case the remaining two d-electrons

occupy the non-bonding d_{xy}-orbital forming a stable complex. This cation is then available for the nitrate anion to coordinate. A reasonable bonding situation of the nitrato-complex **Int2** is shown in Figure 11, which allows for a subsequent breaking of the nitrogen-oxygen bond. There π-backbonding from the HOMO of the metal-complex to the antibonding π-orbital of the nitrate loosens the oxygen-nitrogen bond, as is the case for the σ-bonding from the bonding σ-orbital of the nitrate to the empty $d_{x^2-y^2}$-orbital. The braking of the oxygen-nitrogen-bond results in the formation of the d^0 dioxo-complex **3**. This cationic complex is then reduced by dimethyl sulfide (DMS), which is used in this work as terminal oxygen-acceptor. The dissociation of the dimethyl sulfoxide (DMSO) closes the catalytic cycle.

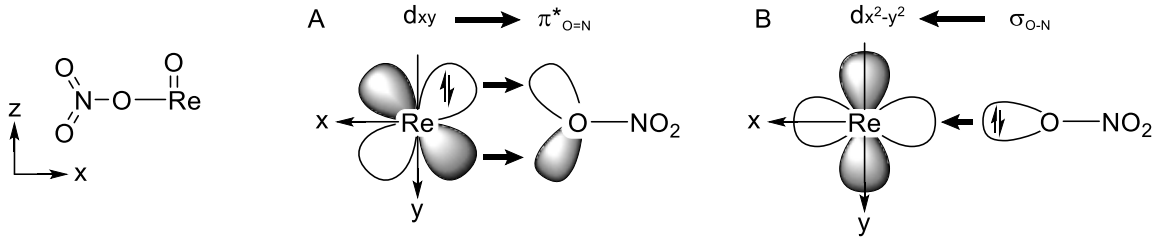

Figure 11 Suggested stereoelectronic situation in **Int2** that leads to the breaking of the oxygen-nitrogen bond A) π-backbonding form the dxy-orbital to the antibonding π-orbital of the nitrate B) σ-bonding from the σ-bonding orbital of the nitrate to the dx^2-y^2-orbital of the metal

When an equimolar amount of $(Bu_4N)NO_3$ is added to a solution of **2** and three equivalents of DMS in dry acetonitrile under inert conditions, the full conversion of one equivalent DMS to DMSO can be observed by ^{1}H NMR spectroscopy after several hours. After the first equivalent of DMS is converted, oxidation slows down drastically and subsequent oxidation of an additional half equivalent DMS to DMSO occurs over roughly 250 hours. This observation indicates that reduction of nitrate and the OAT to sulfide happens on a rather short time scale compared to whatever DMS oxidation that takes place afterwards. Those distinct time scales also imply that nitrate reduction happens first, which allows to investigate it separately from its follow-up reactions. When the experiment is performed without the exclusion of air and moisture, the nitrate reduction appears to happen on a similar time scale as in the inert case. However, subsequent DMS oxidation beyond one equivalent seems to be much faster than under inert

conditions. This different behavior under atmospheric conditions will be discussed in chapter 2.2. The progress of DMS conversions using different oxygen donors under the same conditions in catalytic experiments is shown in Figure 12.

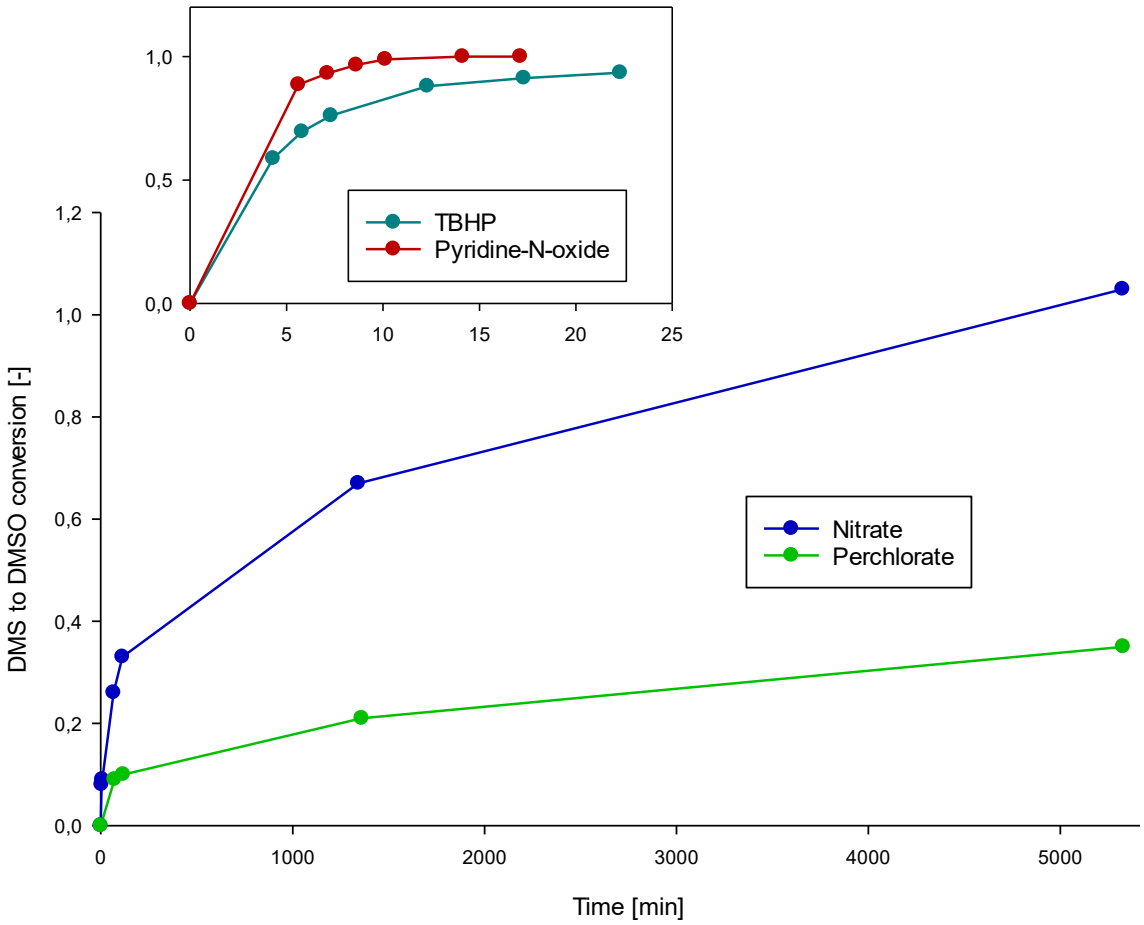

Figure 12 Progression of the DMS to DMSO conversion when 10 equiv. oxidant (TBHP, pyridine-N-oxide, $(Bu_4N)NO_3$ and $(Bu_4N)ClO_4$) and 12 equiv. DMS are added to a 6.9 mM solution of **2** in d^3-acetonitrile; DMS conversion was observed via ^1H NMR spectroscopy; TBHP and pyridine-N-oxide reach full turnover after several minutes, whereas the nitrate and perchlorate salt proceed on a time-scale of several days

The rate of DMSO generation is strongly dependent on the oxidant used. *tert*-Butylhydroperoxide (TBHP) and pyridine-N-oxide reach the stoichiometric turnover of one equivalent DMS to DMSO after several minutes, whereas the nitrate and the perchlorate salt proceed on a time-scale of several days. Those different reaction rates exclude the sulfoxidation (OAT from **3** to sulfide) as being the turnover-limiting step, because otherwise the reaction rates would be the

same with all the different oxidants used. They also exclude the formation of **Int1** (loss of the chloro-ligand resulting in a cationic complex) from being the turnover-limiting step for the same reasons. If the formation of **Int2** would be turnover-limiting, an inverse behavior could be expected because the anionic perchlorate and nitrate should bind more readily to the cationic species **Int1** than the neutral pyridine-N-oxide and TBHP. From those considerations it can be concluded that the turnover-limiting step in the catalytic cycle shown in Figure 10 is most certainly the breaking of the substrate-oxygen bond resulting in the formation of the dioxorhenium(VII) cation **3**, so the OAT from the substrate to the metal-catalyst. This is consistent with theoretical investigations on similar systems[11] and on this one.[77] In none of those catalytic experiments a species other then **2** was visible in the ^{1}H NMR spectra during catalytic sulfoxidation. This indicates that the equilibrium between **2** and **Int1** either lies strongly on the side of **2** or that intermediate **Int1** is not formed at all, and nitrate directly substitutes the chloro ligand in an associative mechanism without the initial dissociation of the chloro ligand.

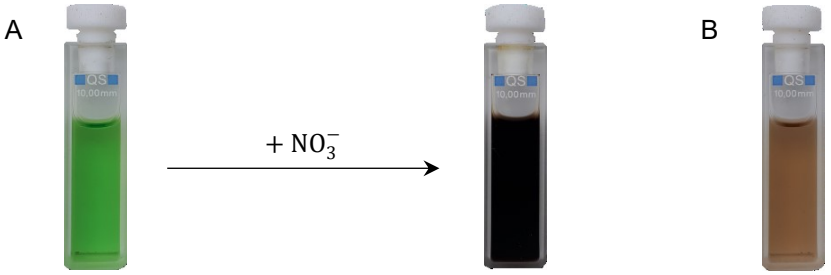

Figure 13 A) **2** dissolved in acetonitrile (green, 5 mmol/L) changes color to dark brown when an excess of nitrate is added B) Dark brown solution of A diluted 1:50 to give a better optical impression

Solutions of **2** in acetonitrile are light green. Generally when an oxygen donor, such as TBHP, perchlorate or nitrate is added, those light green solutions turn dark brown (Figure 13). This color-change of oxorhenium(V) complexes has already been subject to extensive kinetic studies, where so far it was assigned to the formation of the dioxorhenium(VII) compound as shown in Figure 3.[11,73] Although this brown species is assumed to be the dioxorhenium(VII) cation, there is so far no further evidence which would support this claim. When no efforts are made to exclude air and moisture, this brown color fades over time resulting in a

clear, colorless solution. This discoloration is thought to be a result of the hydrolysis of the dioxorhenium(VII) cation, which shall be discussed later on in chapter 2.1.3.[11,73]

2.1.1 Formation of the oxidation product

Figure 14 shows the UV/Vis spectrum of **2** before and after an excess of nitrate is added. Accompanied with the color-change from light green to brown, a shoulder at 540 nm appears. This shoulder in combination with the high extinctions in the lower wavelength-region results in a brown, reddish color. Consequently further investigations towards the formation and the decay of the brown compound were performed at 540 nm.

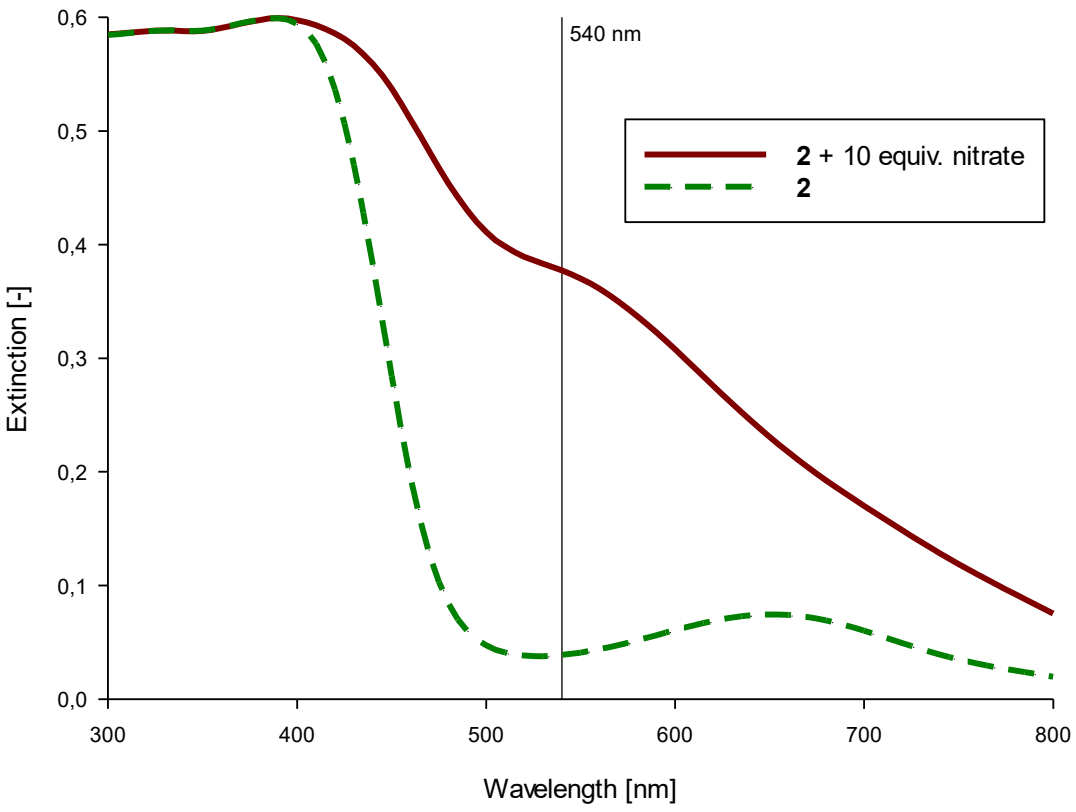

Figure 14 1.5 µmol/L solution of **2** before and 30 min after the addition of 10 equiv. $(Bu_4N)NO_3$; the light green solution turned brown with a shoulder growing at 540 nm

The formation of the oxidation product upon addition of nitrate is followed by its rather slow decay (as shown in Figure 31), supposedly by hydrolysis, within

hours. Following the formation and the subsequent decay of this brown compound under pseudo-first order conditions, the rate-constants, as given in Table 3, were obtained. The Arrhenius-plot as depicted in Figure 15 gives an activation energy for the formation of the oxidation product of E_{A1} = 65 ± 2 kJ mol^{-1} (15.5 ± 0.4 kcal mol^{-1}) and a pre-exponential factor of A_1 = 8 ± 7 x 10^7 s^{-1}. This activation energy is in line with reported values for a similar system using different oxygen-donors. For Abu-Omar's complex (Figure 3) the activation energy for this oxidation is reported to be 57 kJ mol^{-1} with chlorate and 68 kJ mol^{-1} for 4-picoline-N-oxide.[11]

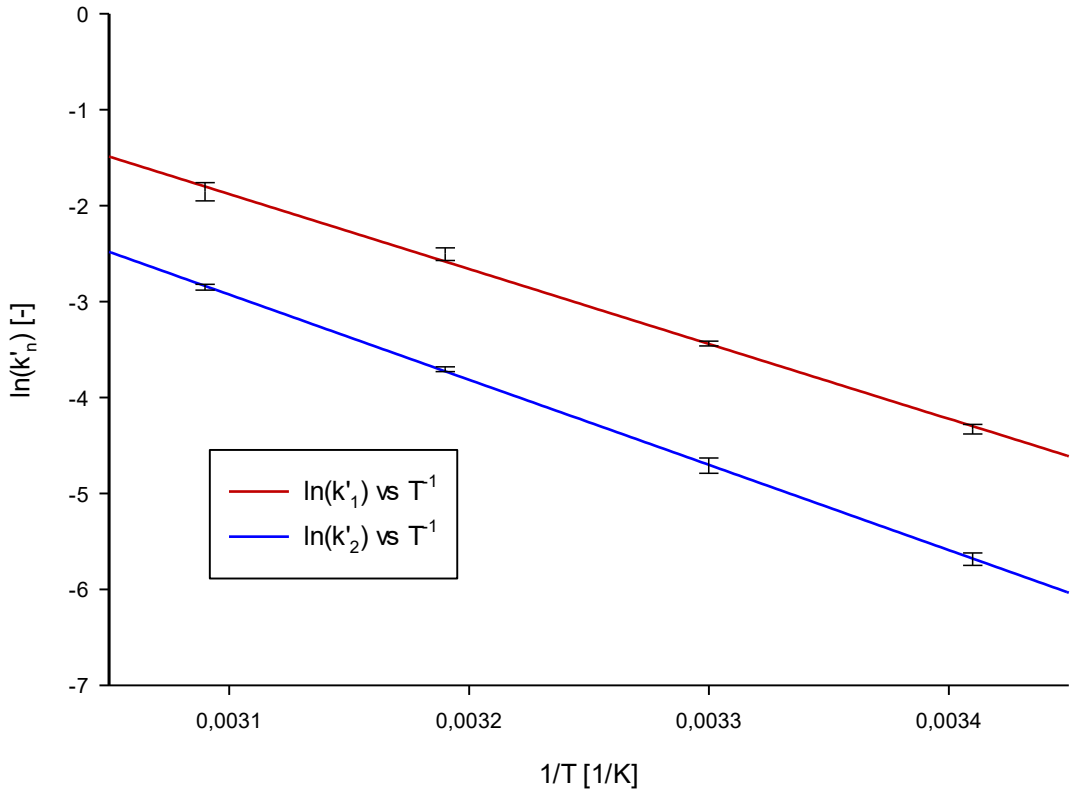

Figure 15 Arrhenius-plot measured by using UV/Vis-spectroscopy (at 540nm and at 50 °C, 40 °C, 30 °C and 20 °C); 100 equiv. of $(Bu_4N)NO_3$ were added to a 0.1 mM solution of **2** in acetonitrile; k'_1 is the pseudo-first-order rate constant for the formation, and k'_2 the pseudo-first-order rate constant for the decay of the oxidation product; the mean-values were omitted for clarity and the error-bars indicate the range within one standard-deviation

2.1.2 What is the oxidation product?

As mentioned above, the oxidation product formed upon addition of an oxygen donor to oxorhenium(V) is assumed to be a dioxorhenium(VII) cation. Various approaches of synthesizing **3** have so far been unsuccessful, but the analogous neutral dioxorhenium(VI) complex **3'** (as shown in Figure 18) is readily available (chapter 2.2.1). As it turned out, the half-wave potential of the **3**/**3'** Re(VII)/Re(VI) redox-couple is in an otherwise empty electrochemical potential-range. Therefore cyclic voltammetry was used to monitor the analogous oxidation reaction as by the UV/Vis-measurements (Figure 16). One of the conclusions from the Randles-Sevcik equation in cyclic voltammetry is the linear dependency of the peak-current with respect to the bulk-concentration of the analyte under otherwise constant conditions.[78]

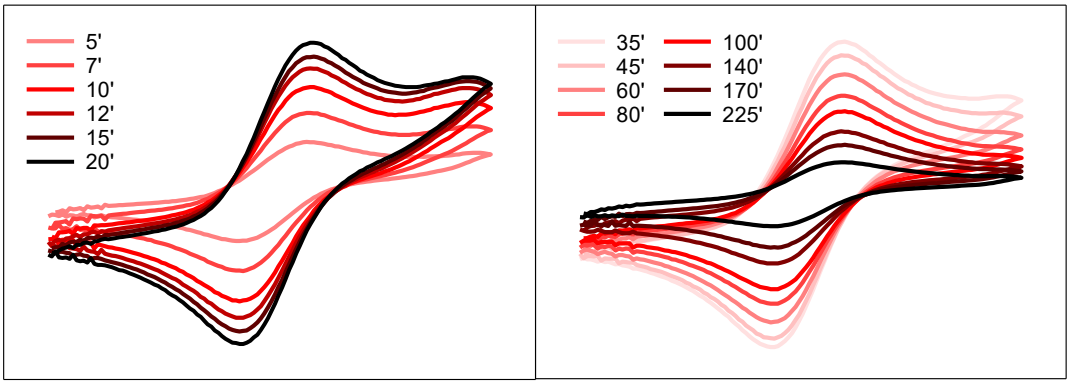

Figure 16 Time resolved cyclic voltammograms of the **3**/**3'** redox-couple at $E_{1/2}$ = 110 mV vs Fc (as in Figure 20) after the addition of 30 equiv. $(Bu_4N)NO_3$ to a 1.0 mM solution of **2** in dry acetonitrile containing 100 mg Bu_4NPF_6 as electrolyte (left: formation of **3**; right: decomposition of **3**)

Evaluation of the peak-current-progression gave again a pseudo-first order rate constant of $k^*_1 = 4 \times 10^{-4}$ s^{-1} at room temperature. The analogous rate constant k'_1 by UV/Vis-measurements obtained from the Arrhenius relationship at 26 °C is k'_1 (299 K) = 4×10^{-4} s^{-1}. The similarity of k^*_1 and k'_1 (299 K) strongly suggests that the oxidation product is indeed the proposed dioxorhenium(VII) cation **3**. Neutral oxorhenium(VI) complex **3'** can be excluded from this considerations as it is light yellow in color and does not absorb light at 540 nm. The pseudo-first

order rate constant for the decay resulting from the CV measurement is k^*_2 = 1.6 x 10^{-4} s^{-1} at room temperature. Although it seems larger compared to the one obtained by the UV/Vis-measurements (k'_2 (299 K) = 9 x 10^{-5} s^{-1}), the number is well within the estimated error of the Arrhenius-prediction of ± 9 x 10^{-5} s^{-1}. Therefore, the similarity of the pseudo-first order rate constants for the decay indicates **3** as the oxidation product.

2.1.3 Fate of the dioxo Re(VII) cation

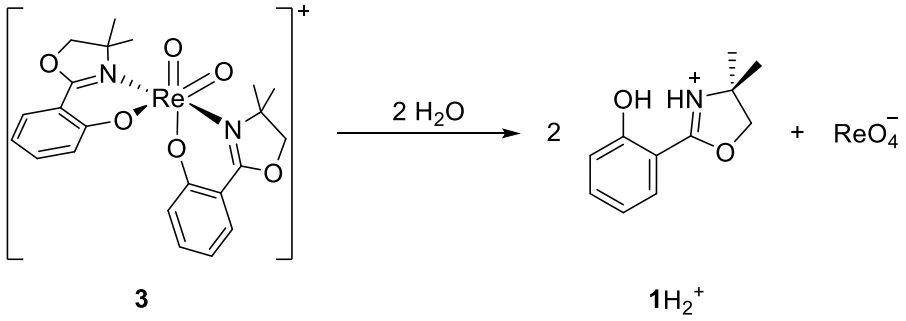

Figure 17 Proposed hydrolysis of the dioxorhenium(VII) resulting in the formation of perrhenate and two equiv. of protonated ligand **1**H_2^+

From the data presented in chapters 2.1.1 and 2.1.2 it can be concluded that cationic dioxorhenium(VII) complex **3** decomposes under atmospheric conditions with the kinetic parameters as given in the Table 3 (see appendix). The Arrhenius parameters obtained for this decay give an activation energy of E_{A2} = 74 ± 1 kJ mol^{-1} (17.7 ± 0.2 kcal mol^{-1}) and a pre-exponential factor of A_2 = 8 ± 4 x 10^8 s^{-1}. The rate constant of this decomposition at room temperature is estimated at around 10^{-4} s^{-1}. FT-IR measurements of the colorless residues from the reaction of **2** with $(Bu_4N)NO_3$ strongly suggest the formation of perrhenate, as a strong peak at 900 cm^{-1} is observed, corresponding to $[ReO_4]^-$.[79,80] The ^{1}H NMR-spectrum of the colorless residue in CD_3CN shows only one set of signals which differs from the free ligand **1**H and is assigned to the protonated ligand **1**H_2^+. This again supports the complete decomposition of **3**. If there would be just a loss of one ligand, at least two sets of signals would be expected. Both these observations are in line with the decomposition by hydrolysis (Figure 17) as proposed for those cationic dioxorhenium(VII) systems by Abu-Omar.[11,73]

2.2 Reactivity regarding nitrite

Similar to the nitrate reducing step, an analogous reaction mechanism (cf. Figure 10) can be proposed. In contrast to nitrate reduction, where the product is simply the nitrite anion, the formation of the NO^n (n = +1, 0, -1) moiety from nitrite-deoxygenation in principle can lead to several products. Possible outcomes are shown in Figure 18.

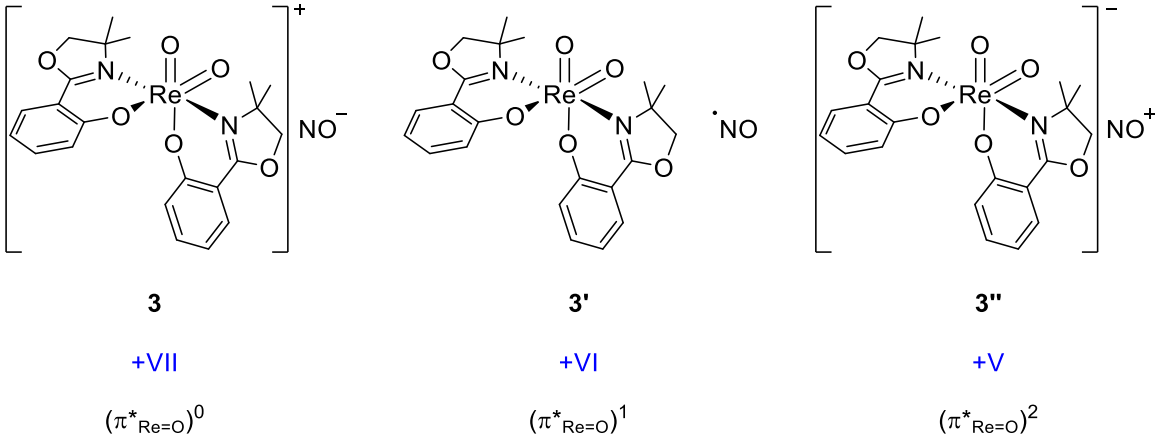

Figure 18 Possible products of the oxidation of **2** by nitrite, the oxidation states of the metal complexes and their electronic configuration (cf. Figure 8)

Although the formation of cationic **3** results in a stable complex from an electronic point of view (none of the antibonding d-orbitals are occupied), the accompanying nitroxyl-anion is a rather unstable species, which is itself not stable under atmospheric conditions and room temperature. So far, no salts of the type MNO, where M is an alkali-metal, are known.[3] The other extreme case would be the formation of anionic complex **3''**. While NO^+ is known to be stable in many compounds,[3] both d-electrons of hypothetical **3''** would occupy the lowest lying antibonding $\pi^*_{Re=O}$-orbital, which leads to an unfavorable electronic situation. The formation of neutral nitric oxide NO and neutral **3'** seems to present a compromise of the stability issues. On the one hand the single remaining d-electron in **3'** occupies an antibonding $\pi^*_{Re=O}$-orbital, which is also an unfavorable electronic situation, the generated nitric oxide on the other hand is a generally stable gaseous molecule, especially when kept under inert, anaerobic conditions.[3] Nitric oxide is also a common intermediate in the biological

denitrification where it is generated from the reaction of nitrite with an oxo-molybdenum(IV) based enzyme, also resulting in a d^1-complex (vide supra). Indeed the reaction of **2** with an excess of $NaNO_2$ suspended in dry acetonitrile under inert conditions and recrystallization from toluene/n-heptane gives fine orange needle-shaped crystals of **3'** (Figure 19). The consequences of the generated nitric oxide shall be discussed later on.

2.2.1 The Re(VI)-dioxo complex **3'**

The structure of the neutral ReO_2(**1**)$_2$ **3'** as shown in Figure 19 was determined by X-ray diffraction analysis. Both ligands occupy positions with a C_2 symmetry, whereby the two-fold axis of symmetry lies between the oxo ligands and the phenolate-oxygens. Selected parameters are presented in Table 1.

Table 1 Selected bond lengths and angles of **3'**

Bond length [Å]		Angles [°]	
Re1-O1	1.7372(10)	O2-Re1-O1	109.24(5)
Re1-O2	1.7329(10)	N13-Re1-N33	169.11(4)
Re1-O21	2.0605(10)	O21-Re1-O41	78.85(4)
Re1-O41	2.0873(9)		
Re1-N13	2.1101(10)		
Re1-N33	2.0929(10)		

The Re-oxo bond-lengths of 1.7372(10) Å and 1.7329(10) Å are within the range of previously reported Re(VI)-dioxo complexes (1.797 Å to 1.741 Å).[81] Comparison of the bond-lengths with similar known Re(VII)-dioxo complexes (1.717 Å and 1.712 Å)[11] show their elongation in the Re(VI) cases because of the occupation of an antibonding $\pi^*_{Re=O}$-orbital by the remaining d-electron. The angle of 109.24(5) between the oxo ligands nearly matches the tetrahedral angle of 109.5°, which highlights the repulsive character of the oxo-moieties. The angles between the oxo ligands and the phenolate groups *trans* to these oxo ligands are 164.13(4)° and 164.73(4)°. The deviations from linear 180° are a result of the strong *trans*-influence of the oxo ligands and allow the phenolate-groups to avoid those *trans*-positions. This strong *trans*-influence is also highlighted by the rather long Re-phenolate distances of 2.0605(10) Å and 2.0873(9) Å.

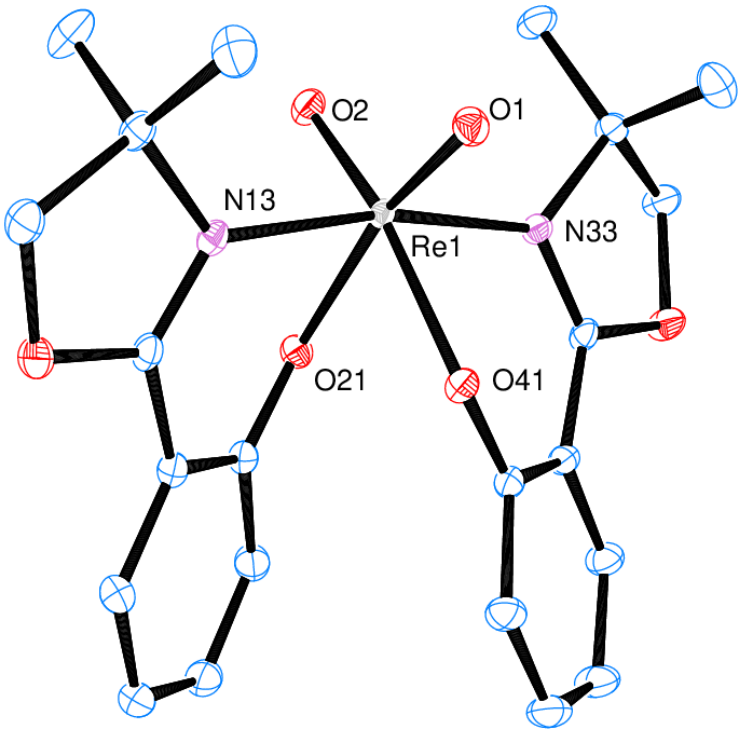

Figure 19 Molecular structure of **3'** (50% probability level, H-atoms and solvent-molecule omitted for clarity)

Figure 20 shows the quasi-reversible redox-couple of **3'**. With an $E_{1/2}$ of 110 mV in acetonitrile, **3'** can be classified as a medium oxidizing and a weak reducing agent with a redox-potential between that of molecular chlorine and bromine.[82] In contrast to known Re(VI)-dioxo complexes the $E_{1/2}$ of **3'** is relatively low.[81] This comparably low half-wave potential indicates that the corresponding Re(VII)-dioxo complex **3** should be rather stable from a thermodynamic point of view, which seems reasonable considering that during the oxidation of **3'** to **3** an electron is removed from an antibonding $\pi^*_{Re=O}$-orbital. Variation of the scan-rate did not significantly affect the ratio of the anodic and the cathodic peak indicating a rather long-lived oxidized species **3**, which is in line with the measurements summarized in chapter 2.1.2.

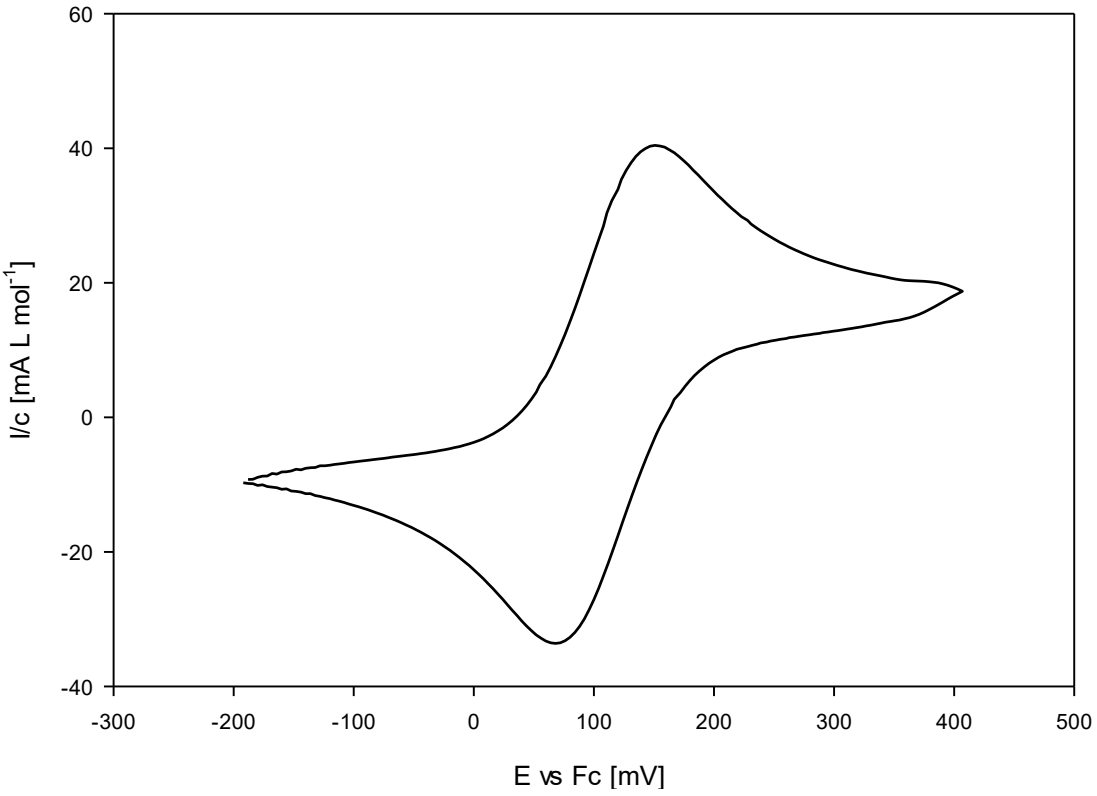

Figure 20 Cyclic voltammogram of **3'** in dry acetonitrile at a scan rate of 500 mV s^{-1}; quasi-reversible redox-couple at $E_{1/2}$ = 110 mV vs Fc

Complex **3'** is in contrast to **3** not capable of sulfoxidation, at least not on a time scale of several hundred hours. On the one hand this seems surprising because its remaining d-electron occupies an antibonding $\pi^*_{Re=O}$-orbital, so the OAT should be favorable. On the other hand the resulting Re(IV) d^3-oxo-complex would also require the occupation of an antibonding $\pi^*_{Re=O}$-orbital, which is again not favorable from an electronic point of view. Therefore, because of its observed inability of sulfoxidation, **3'** can be considered catalytically inactive.

2.2.2 Decomposition of **3'**

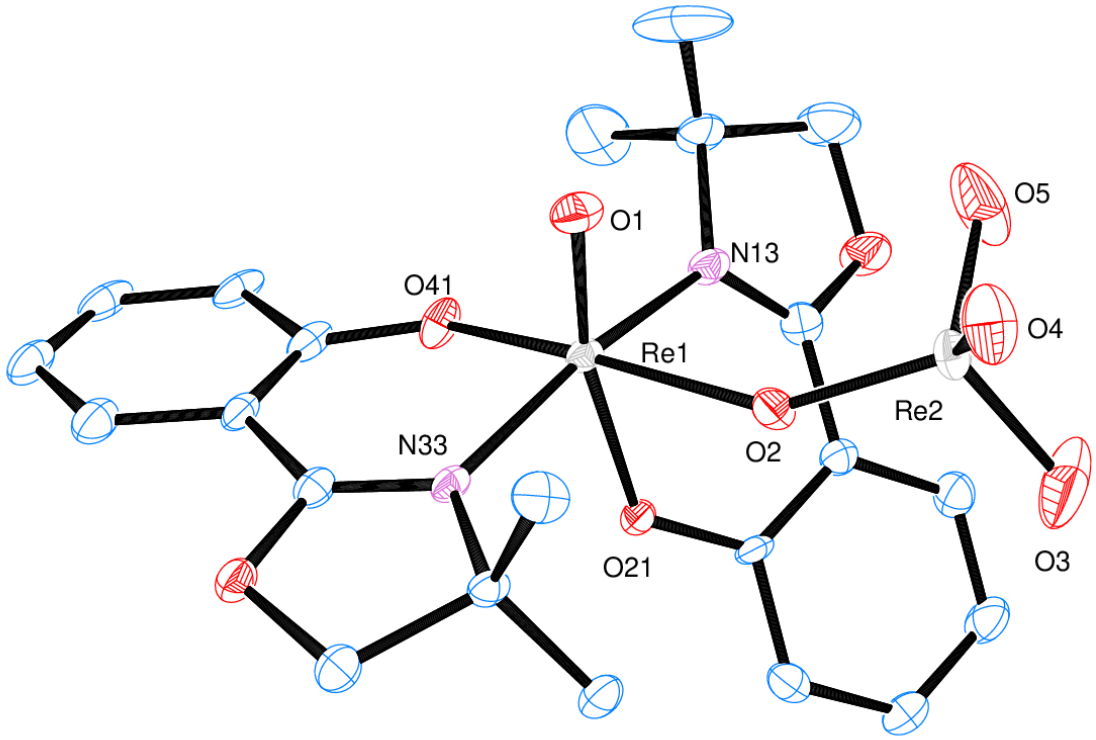

Figure 21 Molecular structure of the decomposition product **4** (50% probability level, H-atoms omitted for clarity)

After being stored for several days **3'** hydrolyses, accompanied by a redox disproportionation. Recrystallization of the decomposition products from dichloromethane/n-heptane gave dark green crystals. X-ray diffraction analysis identified the decomposition product as $[ReO_2(\mathbf{1})_2]ReO_4$, further denoted as complex **4**. The Re(V) moiety is structurally quite similar to catalyst **2**, but with a perrhenate anion coordinated *cis* to the oxo ligand instead of the chloro ligand in **2**. The comparison in Table 2 shows that the Re=O bond length in the oxorhenium(V) complex **4** is basically the same as in the investigated catalyst **2**. This short Re=O bond length highlights its triple bond character resulting from the MO-scheme as shown in Figure 8 for a d^2 complex. Also the distances between Re1 and the surrounding atoms of the phenolate-oxazoline ligands are similar to the ones reported for complex **2**.

Table 2 Comparison of selected bond length of complex **2** (X = Cl1) and **4** (X**=** O2)

Bond length [Å]	**2**[67]	**4**
Re1=O1	1.682(6)	1.682(3)
Re1-O41	1.944(7)	1.965(3)
Re1-O21	2.056(7)	1.984(3)
Re1-N13	2.203(5)	2.120(4)
Re1-N33	2.058(5)	2.082(3)
Re1-X	2.440(2)	2.139(3)
Re2-O2		1.769(3)
Re2-O3		1.704(4)
Re2-O4		1.704(3)
Re2-O5		1.706(4)

Comparison of the Re-O bond lengths around Re2 in the perrhenate moiety shows no significant deviation from reported perrhenate bond length of 1.69 Å to 1.74 Å.[83] This indicates that this perrhenate moiety can indeed be considered a coordinated perrhenate anion rather than a part of a binuclear μ-oxo-bridged complex.

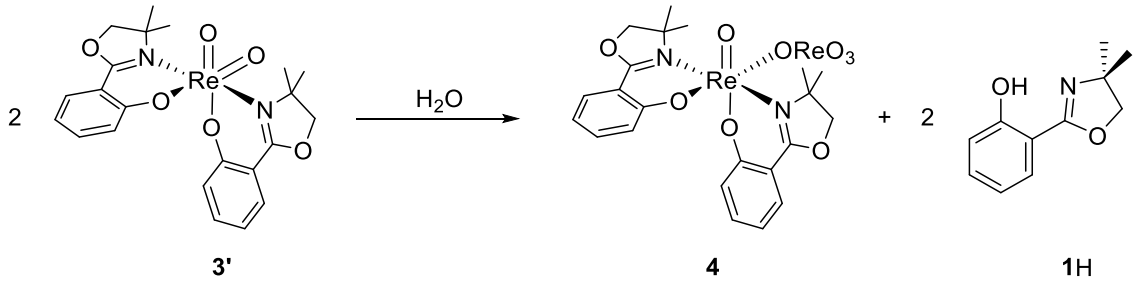

Figure 22 Proposed hydrolysis and redox disproportionation of **3'** to give **4** and **1**H

The decomposition of **3'** to **4** is proposed to occur via hydrolysis as shown in Figure 22. When the decomposition products are dissolved in CD_3CN, the ^1H NMR shows a spectrum which is essentially identical to isolated cationic $[ReO(\mathbf{1})_2]^+$. In addition 2 equiv. of free ligand **1**H can be identified, which would be the expected stoichiometry of a hydrolysis as proposed in Figure 22. The loss of the perrhenate anion upon dissolving **4** in acetonitrile indicates a labile Re1-O2 bond. This is also indicated by the bond length shown in Table 2, where the Re1-O2 bond is significantly longer than the O2-Re2 bond. In contrast to the chloro ligand in **2**, perrhenate readily dissociates when **4** is dissolved in acetonitrile. Therefore perrhenate in **4** presents itself as a more labile ligand than

chloro in **2**, despite the Re1-O2 bond being shorter than the Re-Cl bond in **2**. The decay of **3'** was monitored via UV/Vis-spectroscopy at room temperature in an acetonitrile solution containing 5% H_2O. It confirms a pseudo-first order kinetic for the decay and suggests a half-life time of complex **3'** of 86 h. The half-life time of **3** at room temperature in pure acetonitrile is roughly 2 h. This difference of their half-life times again highlights the stability of the neutral dioxorhenium(VI) complex **3'** compared to the cationic dioxorhenium(VII) complex **3**. The electronic situation in **3'** can be hypothesized to be responsible for its higher stability compared to **3**. When the hydrolysis of **3** is considered, the d^0 configuration of this cationic dioxorhenium(VII) complex results in a singlet spin-state, so does the d^0 configuration of the decomposition product perrhenate ReO_4^-. Therefore the reaction is in principle spin-allowed. In the case of the hydrolysis of **3'**, the d^1 configuration of this neutral dioxorhenium(VI) complex leads to a doublet spin-state, whereas also here the products occupy singlet spin-states. In contrast to the hydrolysis of **3** the decomposition of **3'** should be spin-forbidden because it would require a change of the spin-state. The fact that hydrolysis of **3'** occurs anyway can be justified by significant spin-orbit coupling in second- and especially third-row transition metals, which facilitates transitions between different spin-states.[84]

2.2.3 Consequences of nitric oxide formation

In chapter 2.1 it was described that when an equimolar amount of nitrate and three equivalents of DMS are added to a solution of **2** in acetonitrile, the conversion of the first equivalent of DMS to DMSO basically proceeds equally fast, no matter if the reactions are carried out under inert or atmospheric conditions. This initial conversion is associated with the reduction of nitrate to nitrite. After that the behavior under the two different conditions, inert or atmospheric, diverges. Under inert conditions further DMS to DMSO conversion proceeds extraordinary slow, whereas under atmospheric conditions this conversion appears to happen on a time scale similar to the initial conversion. This behavior can be best explained with the initial formation of nitric oxide NO as the reduction product of nitrite. As mentioned in chapter 1.4, nitric oxide reacts

quite readily with oxygen to form NO_2. Nitrogen dioxide is itself known to be a potent oxidizing agent and was therefore investigated regarding its reactivity with **2** and DMS.[3] When a green solution of **2** in acetonitrile is stirred under an NO_2 atmosphere, it undergoes the same color-change than with other oxygen-atom donors like nitrate, perchlorate or TBHP (as shown in Figure 13). This would be in line with an OAT from the nitrogen dioxide to the metal complex resulting again in the formation of nitric oxide and cationic complex **3**. Although the oxidation of DMS to DMSO using NO_2 is well known and even used in industrial applications[85], the behavior of DMS under nitrogen dioxide atmosphere without complex **2** was investigated. Roughly 0.5 equivalents of NO_2, estimated by its volume using the ideal gas law, was bubbled through a solution of 1.0 equivalent of DMS in d^3-acetonitrile in an NMR-tube, which was quickly sealed afterwards. After several hours, full conversion of DMS to DMSO was determined, instead of a 50/50 mixture of DMS/DMSO, as dictated by the chosen stoichiometry. Because this experiment was performed under atmospheric conditions, the generated nitric oxide was re-oxidized to NO_2 by atmospheric O_2, which finally lead to the observed full conversion of DMS to DMSO after several days (the NMR-tube remained sealed). Those observations can be summarized by a parallel catalytic system as shown in Figure 23.

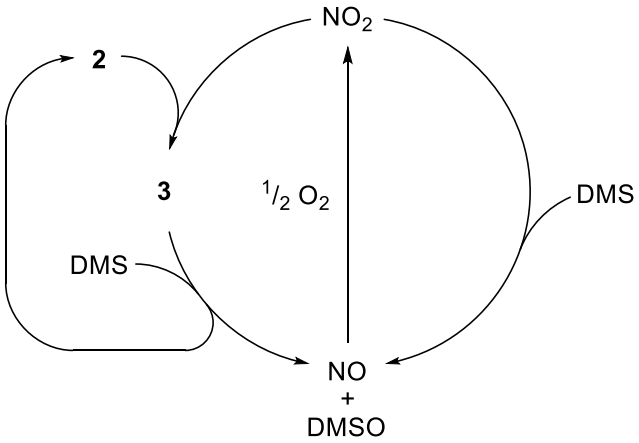

Figure 23 Interfering behavior of the nitric oxide under atmospheric conditions resulting in the conversion of DMS to DMSO

In the presence of oxygen and NO/NO_2 a conversion of DMS to DMSO can be observed, with and without the presence of **2**. Observing the DMS oxidation is

therefore an insufficient method for studying the catalytic behavior of **2** and similar systems regarding nitrate degradation under atmospheric conditions! Under inert conditions the formed nitric oxide is obviously not able to react with molecular oxygen to the nitrogen dioxide. As mentioned in chapter 1.4 nitric oxide can undergo disproportionation according to 3 NO → NO_2 + N_2O. Again NO_2 is generated which can again react with DMS as shown in Figure 23. This leads to a repetitive reaction scheme as depicted in Figure 24.

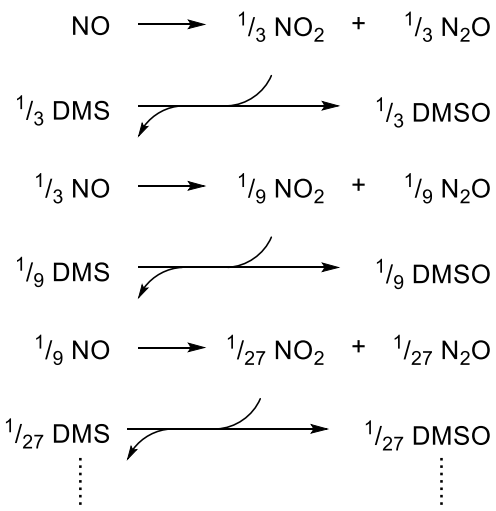

Figure 24 Reaction scheme of NO disproportionation and the following reaction with DMS

The equivalents DMSO generated of one equivalent nitric oxide form a geometrical series whose partial sums converge towards 0.5 equiv.:

$$\text{equiv. DMSO} = {}^1/_3 + {}^1/_9 + {}^1/_{27} + \ldots = ({}^1/_3)^1 + ({}^1/_3)^2 + ({}^1/_3)^3 + \ldots = (1-{}^1/_3)^{-1} - 1 = {}^1/_2$$

Analogously, also 0.5 equiv. nitrous oxide N_2O are generated. This would subsequently lead to the conversion of nitric oxide to nitrous oxide N_2O and the oxidation of half an equivalent DMS to DMSO according to the net reaction 2 NO + DMS → N_2O + DMSO. The reduction of NO to N_2O is supported by ^{15}N NMR measurements, where one equivalent of labeled $^{15}NO_3^-$ was added to one equivalent of **2** and two equivalents of DMS under inert conditions. After several hours, shifts for $^{15}N_2O$ were observed in the ^{15}N NMR spectrum as the only diamagnetic ^{15}N containing species. The ^1H NMR spectrum after that time displayed a DMS conversion of only 0.8 equivalents and the formation of the

paramagnetic complex **3'**.[86] In Figure 25 the progress of DMSO generation in a reaction of **2** with an equimolar amount $(Bu_4N)NO_2$ and three equivalents of DMS is shown.

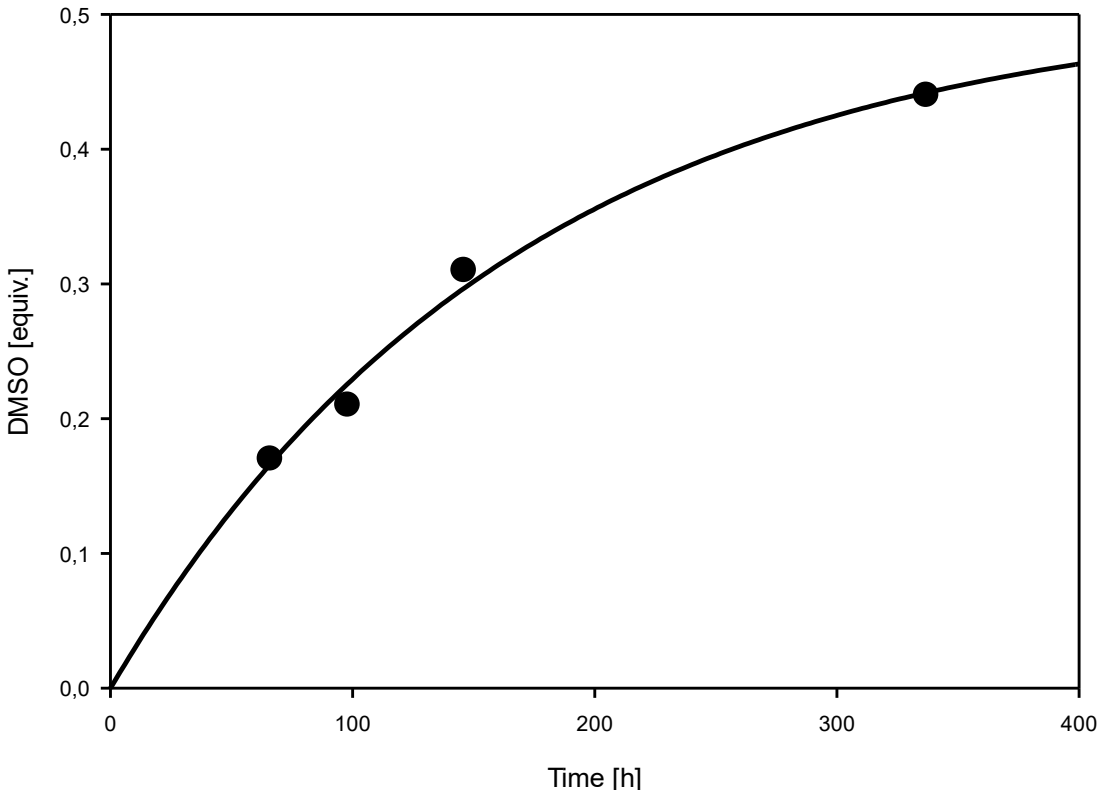

Figure 25 1 equiv. **2** + 1 equiv. $(Bu_4N)NO_2$ + 3 equiv. DMS were mixed under inert conditions in an J-Young NMR-tube which was sealed immediately afterwards; non-linear fit of an exponential increase suggests a boundary value of 0.51±0.03 equivalents DMSO generated with respect to the nitrite added

The non-linear fit for the exponential increase suggests a boundary value for the DMS conversion of 0.51 ± 0.03 equivalents, which again supports the hypothesized disproportionation of nitric oxide that would result in a DMS conversion of 0.5 equivalents. Although this conversion proceeds on a rather slow time scale of some several hundred hours, the uncatalyzed disproportionation of nitric oxide NO to nitrous oxide N_2O and nitrogen dioxide NO_2 at 298 K and 1 atm would take years.[87] If the observed N_2O is indeed the product of NO disproportionation, then the extreme rate acceleration can only be caused by a catalyst, which is in this case most certainly a rhenium complex. Such transition-metal catalyzed disproportions are well known and have the, at least intermediate, formation of nitroso-complexes in common.[88,89] When a solution of

2 in acetonitrile is stirred under an inert NO atmosphere, the solution turns from initial green to yellowish dark brown over two weeks. After purging the flask and removing the solvent by vacuum a dark brown solid remains. The ^{1}H NMR spectrum in CD_3CN shows paramagnetic signals at δ [ppm]: 11.9 (bs), 11.0 (bs), 10.1 (bs), 9.9 (bs), 9.0 (bs), which are different from **3'**. Assuming a coordination of the nitric oxide radical to the d^2 complex **2**, an odd-numbered, and therefore paramagnetic, nitrosyl complex would result. Apparently the reaction of $ReOX_3L_2$ with NO is reported to be a commonly used synthetic pathway to $Re(NO)X_3L_2$ complexes.[90] Starting from $ReOX_3(PPh_3)$, numerous examples of this reaction are known.[91–94] It is therefore possible that the reaction of $ReOCl(\mathbf{1})_2$ (**2**) with NO also follows a reduction and deoxygenation of the oxorhenium(V) complex **2**. The hypothetical product would be $Re(NO)Cl(\mathbf{1})_2$. This species would have a d^5 configuration and therefore would also be paramagnetic, which again would be in line with ^{1}H NMR measurements. The formation of this hypothetical $Re(NO)Cl(\mathbf{1})_2$ complex would represent a decomposition of the oxorhenium(V) catalyst **2**. Despite that, this experiment shows that **2** is potentially capable of interacting with NO, which is an essential property for further catalytic degradation of NO, for instance to N_2O.

2.2.4 Investigation of the volatile products

In order to prove that gaseous nitric oxide is formed in the reaction of nitrite and **2**, the volatile components of several reactions were investigated under different conditions. For the experimental procedure see chapter 4.4. As a reference reaction three equivalents of nitrate were added to a solution of **2** under inert conditions. After several hours the volatile compounds contained within the reaction flask were condensed and trapped in a second flask, cooled to -100 °C, containing four equivalents of DMS in d^3-acetonitrile. Even after 100 hours no significant DMS conversion occurred, which is expected, because the reaction of nitrate with **2** results in the formation of nitrite, a non-volatile compound. This experiment was repeated analogously under inert conditions with an excess of KNO_2 added to a solution of **2** and the volatile compounds were trapped at -196 °C. After 12 hours, ^{1}H NMR experiments showed roughly 0.5 equivalents

DMS were oxidized to DMSO, but over the next 230 hours, no further DMS oxidation took place. Under ideal oxygen-free conditions, only the formation of NO would be expected, which itself is not capable to oxidize DMS. The observed small conversion of DMS must have been effected by traces of NO_2, itself the oxidation product of NO and O_2. Traces of oxygen must therefore have been present in the experimental set-up, beside best efforts. Such traces of oxygen could be present in the non-degassed DMS that was used or in the pre-dried nitrite salt. Nevertheless, after those 230 hours, the J-Young NMR-tube containing the condensed phase was purged with dry O_2, which lead to a further oxidation of roughly another 0.5 equivalents of DMS over the next 120 hours, as expected if nitric oxide is present in the solution. A parallel sample from the same reaction, which was exposed to air immediately afterwards, showed continuous oxidation of DMS. In this sample, after about 300 hours, all four equivalents of DMS were consumed, in line with nitric oxide being initially present in the condensed phase. These experiments are summarized in Figure 26.

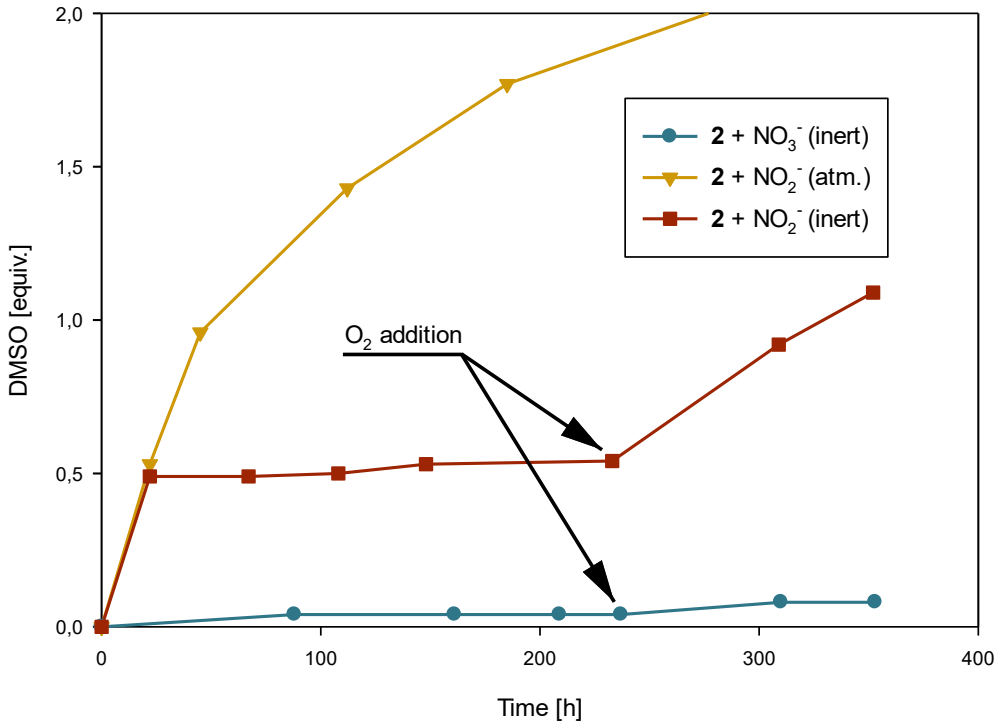

Figure 26 DMS to DMSO conversion when 4 equiv. DMS are added to the trapped volatile compounds generated by the reaction of **2** with $(Bu_4N)NO_3$ (blue) and with $(Bu_4N)NO_2$ (orange: atmospheric conditions, red inert conditions)

Tris-dithiocarbamate-iron- complexes are long known indicators for the presence of nitric oxide. Especially for the detection of nitric oxide in biological surroundings several trisdithiocarbamate-iron complexes were developed.[95,96] The indication of nitric oxide is based on the nitrosylation of the iron complexes accompanied by the loss of one dithiocarbamate ligand. Because the resulting Fe(II)(NO)(dithiocarbamate)$_2$ complexes have an odd number of electrons, this reaction is commonly followed by EPR-spectroscopy.[95–98]

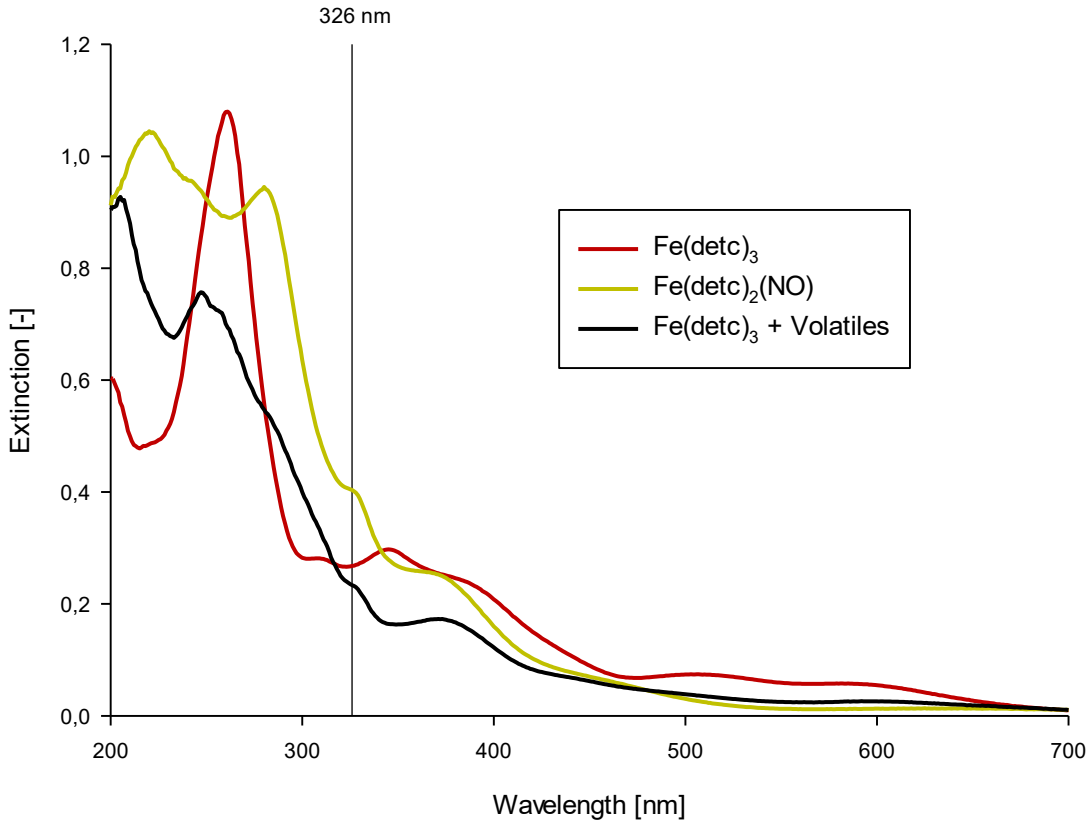

Figure 27 UV/Vis-spectra of 0.03 mM solutions in acetonitrile of Fe(detc)$_3$, the nitrosylation product Fe(detc)$_2$(NO) and the reaction of Fe(detc)$_3$ with the volatile compounds generated by the reaction of **2** with KNO_2

In order to avoid these rather demanding EPR-measurements, tris(N,N-diethyldithiocarbamato)iron(III) (further denoted as Fe(detc)$_3$) was used as an indicator that undergoes a color change upon nitrosylation, that can be conveniently detected by UV/Vis-spectroscopy.[96] Accordingly, the volatile compounds generated by the reaction of **2** with KNO_2 were allowed to react with Fe(detc)$_3$ as described in chapter 4.4. As a reference, Fe(detc)$_3$ was also reacted

with NO and analyzed by UV/Vis spectroscopy. Results of these measurements are summarized in Figure 27. Although the reaction product does not match the nitrosylation-product $Fe(detc)_2(NO)$ completely, especially the shoulder that arises at 326 nm indicates the presence of $Fe(detc)_2(NO)$ in the solution and therefore the formation of volatile nitric oxide in the reaction of **2** with KNO_2. Also the ^1H NMR spectra of the non-volatile residues produced in the experiments using nitrite salts clearly show the generation of **3'**, which is the expected rhenium product if nitric oxide is released.

2.2.5 Reactivity towards N,N-dimethyl-4-nitrosoaniline

N,N-dimethyl-4-nitrosoaniline (further referred to as NOA) was used as a model substrate for the NO fragment generated. In biochemical studies it is generally used as an electron acceptor, where its reduction is reported to lead to the formation of the corresponding hydroxylamine.[99,100] Nitrosoarenes are also used as a stable model for generally unstable HNO.[101,102]

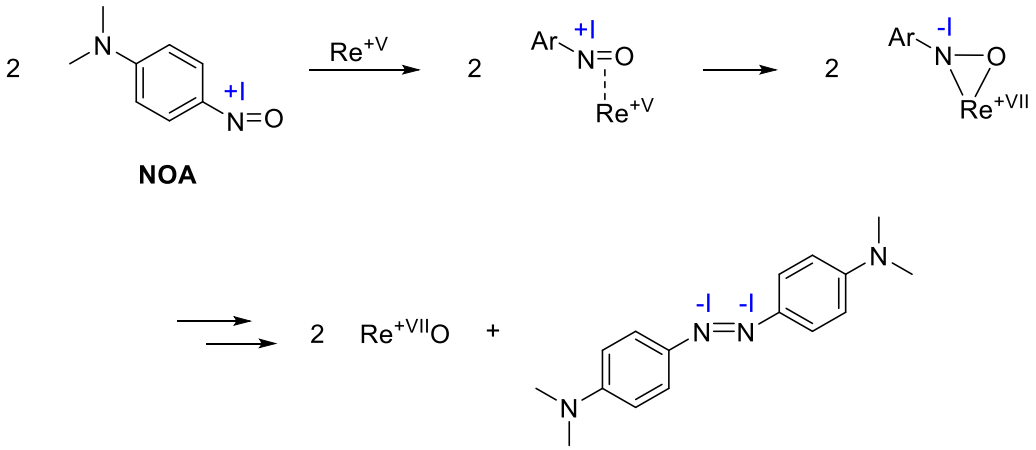

Figure 28 Possible binding scenario of nitroso-aniline compound NOA at the oxorehenium(V) catalyst preceding azo-compound formation

So far no oxorhenium(V) complexes with coordinated nitrosoarenes (ArNO) have been characterized. In oxomolybdenum(IV) complexes these ArNO are known to coordinate side-on *cis* to the oxo ligand to give the (hydroxylamine-O,N)oxomolybdenum(VI) complexes, where geometrical parameters indicate that the double bond of the nitroso group is reduced to a single bond, as in hydroxylamine.[103,104] This situation is shown in Figure 28 analogously for a

possible coordination and reduction of NOA at a Re(V) complex, where the comparison of nitrogen oxidation states show that such a reduction is at some point essential for the formation of the corresponding azo-compound. This suggested azo-coupling is an OAT reaction where the oxygen atom is transferred from the NOA to the metal catalyst.

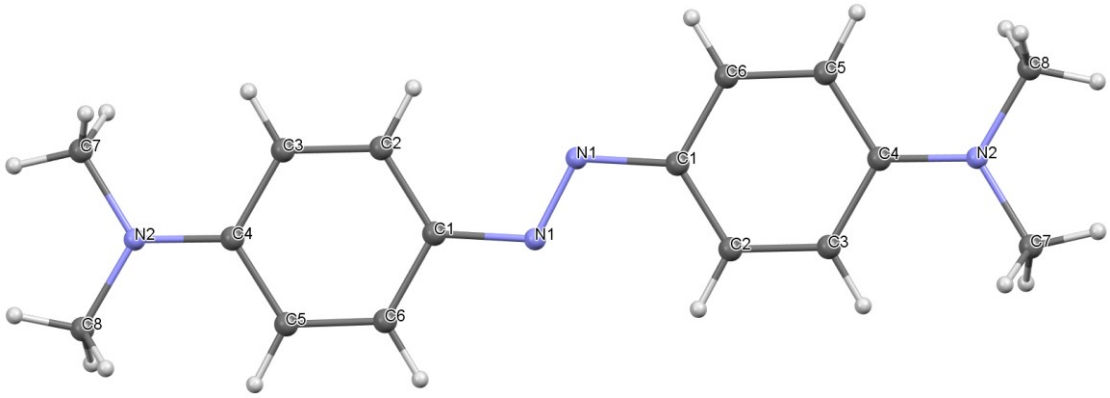

Figure 29 Molecular structure of the reaction product of **Int1** + 2 equiv. NOA, an azo-compound

Two equivalents NOA were allowed to react with the triflate salt of **Int1** in acetonitrile for several hours. In order to isolate just the organic compounds, the reaction mixture was filtered over silicagel. From the resulting solution orange crystals could be obtained. They were identified by X-ray diffraction analysis as the azo-compound shown in Figure 29. It is the formal azo-coupling product of NOA as proposed for the reaction shown in Figure 28. In order to exclude the silicagel from acting as the coupling agent, a solution of NOA in CD_3CN containing silicagel was stirred several minutes. A ^1H NMR spectrum showed no reaction of the NOA in the presence of silicagel. This result indicates that the Re catalyst is needed for the coupling to occur. This experimental observation that an oxorhenium(V) complex catalyzes azo-coupling of NOA is in accord with the known capability of oxometal complexes in high oxidation states to reduce NO-fragments.[103,104] Also catalysis of the disproportionation 3 NO → NO_2 + N_2O (vide supra) seems reasonable because also here at least for the N_2O formation the reduction of an NO educt is essential.

3 Conclusions

Oxorhenium(V) complex **2** was investigated concerning its capability to catalytically reduce nitrate accompanied by the oxidation of the organic sulfide SMe_2 (DMS). The initial step regarding nitrate degradation occurs via an OAT mechanism, where the nitrate initially oxidizes the oxorhenium(V) complex **2**, resulting in the formation of cationic dioxorhenium(VII) complex **3** and nitrite. Subsequently **3** is capable to oxidize DMS to DMSO. This regenerates **2** and therefore closes the catalytic cycle regarding nitrate reduction. In contrast to nitrate, the reaction of **2** with the so generated nitrite does not proceed via a standard two-electron OAT mechanism to again give **3**, but rather a one-electron OAT occurs, which oxidizes **2** to the neutral, paramagnetic dioxorhenium(VI) complex **3'** under formation of singly-reduced nitric oxide NO. Complex **3'** is in contrast to **3** not able to perform sulfoxidation and can therefore not regenerate **2**. When molecular oxygen is present, the formed nitric oxide is oxidized to NO_2 which then is capable of both, sulfoxidation and oxidation of **2** to **3**. Both reactions lead to the formation of nitric oxide again, which then can be re-oxidized to NO_2, as long as molecular oxygen is present. This reaction sequence itself represents a catalytic cycle for the sulfoxidation, with molecular oxygen being the oxidant and NO being the catalyst. Therefore, the use of DMS as a sacrificial oxidant is an impractical method for further investigations, as it leads to false positives. Avoiding the formation of singly-oxidized dioxorhenium(VI) complex **3'** poses the major challenge for the further development of this catalytic system. The observation of $^{15}N_2O$ in the presence of **3'** however might indicate that further reduction activity is preserved in **3'**. Also the reactivity of the catalyst towards nitric oxide, especially the potential formation of a nitrosyl complex, remains an open question for ongoing research.

4 Experimental section

4.1 General

All experiments, if not stated otherwise, were performed using commercially available chemicals and solvents without further purification. Inert experiments were performed under N_2 atmosphere using standard Schlenk- and glovebox techniques. Dry solvents were obtained from a Pure Solv® solvent purification system. UV/Vis-spectra were recorded on a Varian Cary® 50 UV-Vis spectrophotometer. All measurements were performed in 1 cm quartz cuvettes using solutions in acetonitrile. The cuvette-holder was cooled/heated with a cryostat. The evaluation of kinetic studies in order to obtain rate constants was performed within the associated software (Agilent Technologies CaryUV®). Cyclic voltammetry was performed in a glovebox under N_2 atmosphere using a Gamry Instruments Reference® 600 potentiostat. Roughly 1 mM solutions of the analyte were prepared in dry acetonitrile containing 100 mM $(Bu_4N)PF_6$ as supporting electrolyte. Platinum was used as working electrode, Pt wire (99.99%) as supporting electrode and the reference electrode was a Ag wire immersed in a solution of 10 mM $AgNO_3$ and 100 mM $(NBu_4)PF_6$ in acetonitrile separated from the solution by a Vycor® tip. NMR measurements were performed on a Bruker Avance® (300 MHz) instrument and the spectra were referenced to the residual solvent signals. IR-spectra were collected on a Bruker Optics ALPHA® FT-IR spectrometer equipped with an ATR diamond probe head. Structure determination of single crystals using X-ray diffractometric measurements were performed on a Bruker-AXS Smart Apex CCD® diffractometer using monochromatic Mo-K_α radiation at 100 K. Compound **2** was prepared according to literature[67], as well as $Fe(detc)_3$.[105] The reference compound $Fe(detc)_2(NO)$ was prepared by simply stirring a solution of $Fe(detc)_3$ in dry acetonitrile under NO atmosphere.

4.2 Synthesis of **3'**

2 (1 equivalent, 118 mg, 191µmol) was dissolved in 10 ml dry acetonitrile under inert conditions. Pre-dried KNO_2 (2.8 equivalents, 45 mg, 530 µmol) was suspended and the green solution turned dark orange after 5 hours. The solvent was allowed to evaporate on vacuum and the residue was again dissolved in 4 ml dry toluene. This suspension was filtered and the clear dark orange solution was reduced on vacuum to roughly 1 ml. After the addition of 4 ml dry n-heptane an orange precipitate is formed. The supernatant solution is removed and the dark yellow product is dried on vacuum. The synthesis was performed under inert conditions.

ATR-IR: 909 cm^{-1} (m, $Re=O_2$ stretch, sym.); 799 cm^{-1} (s, $Re=O_2$ stretch, asym.)

1H NMR (CD_3CN, 300 MHz) δ [ppm]: 22 (bs), 17.5 (bs), 11.5 (bs), 8.1 (bs), 7.6 (bs), 7.1 (bs), 4.4 (bs)

4.3 Nitric oxide generation

Nitric oxide was generated by adding an equimolar amount of a degassed, aqueous solution of 1 M H_2SO_4 and 1 M $Fe(SO_4)_2.7H_2O$ to $NaNO_2$ or KNO_2 under inert conditions. The formed gas is washed by bubbling it through aqueous 4 M KOH. Subsequently it is dried with concentrated H_2SO_4, 3 Å molecular sieve and dry P_2O_5. Subsequently NO_2 was produced by simply allow air to get in contact with the NO.

4.4 Condensation of volatile compounds

The general setup of those experiments is depicted in Figure 30. Under inert conditions, an excess (generally 2-5 equivalents) of the nitrate or the nitrite salt is added to a solution of **2** in dry acetonitrile or dry CD_3CN (in the left flask in Figure 30). Over several dozens of minutes, the temperature of the reaction was carefully increased up to 90 °C (the system remained closed), until all of the solvent has evaporated and condensed in the cooled flask (the right flask in Figure 30). In order not to lose volatile compounds, no vacuum was applied in

order to accelerate this evaporation. Further reagents, such as DMS or $Fe(detc)_3$, were placed in the cooled flask either before or after starting the reaction. The cooled flask was held at -100 °C or -196 °C.

Figure 30 General setup for the condensation-trapping experiments; the left flask contains the rhenium catalyst, the nitrate or nitrite salt and can be heated in the oil-bath; the right flask contains DMS in CD_3CN and is cooled down, generally to -100 °C or -196 °C, in order to trap volatile compounds generated in the left flask

5 References

(1) Holm, R. H. *Chem. Rev.* **1987**, *87*, 1401–1449.

(2) Atkins, P. W.; Paula, J. de. *Physical chemistry*, 9th ed.; Wiley-VCH: New York, 2010.

(3) Holleman, A. F.; Wiberg, E.; Wiberg, N.; Fischer, G. *Anorganische Chemie*, 103. Auflage; De Gruyter: Berlin, Boston, 2017.

(4) Abu-Omar, M. M.; McPherson, L. D.; Arias, J.; Béreau, V. M. *Angew. Chem. Int. Ed.* **2000**, *39*, 4310–4313.

(5) Rikken, G. B.; Kroon, A. G. M.; van Ginkel, C. G. *Appl. Microbiol. Biotechnol.* **1996**, *45*, 420–426.

(6) van Ginkel, C. G.; Rikken, G. B.; Kroon, A. G. M.; Kengen, S. W. M. *Arch. Microbiol.* **1996**, *166*, 321–326.

(7) Logan, B. E. *Biorem. J.* **1998**, *2*, 69–79.

(8) Kengen, S. W. M.; Rikken, G. B.; Hagen, W. R.; van Ginkel, C. G.; Stams, A. J. M. *J. Bacteriol.* **1999**, *181*, 6706–6711.

(9) Abu-Omar, M. M.; Appelman, E. H.; Espenson, J. H. *Inorg. Chem.* **1996**, *35*, 7751–7757.

(10) Abu-Omar, M. M.; Espenson, J. H. *Inorg. Chem.* **1995**, *34*, 6239–6240.

(11) McPherson, L. D.; Drees, M.; Khan, S. I.; Strassner, T.; Abu-Omar, M. M. *Inorg. Chem.* **2004**, *43*, 4036–4050.

(12) Ahn, Y.-H. *Process Biochem.* **2006**, *41*, 1709–1721.

(13) Canfield, D. E.; Glazer, A. N.; Falkowski, P. G. *Science* **2010**, *330*, 192–196.

(14) Colliver, B. B.; Stephenson, T. *Biotechnol. Adv.* **2000**, *18*, 219–232.

(15) Wasser, I. M.; Vries, S. de; Moënne-Loccoz, P.; Schröder, I.; Karlin, K. D. *Chem. Rev.* **2002**, *102*, 1201–1234.

(16) Carreira, C.; Pauleta, S. R.; Moura, I. *J. Inorg. Biochem.* **2017**, *177*, 423–434.

(17) Moura, I.; Moura, J. J. G.; Pauleta, S. R.; Maia, L. B. *Metalloenzymes in Denitrification*; Royal Society of Chemistry: Cambridge, 2016.

(18) Nicholas, D. J.; Nason, A. *J. Biol. Chem.* **1954**, *207*, 353–360.

(19) Nicholas, D. J.; Nason, A.; McElroy, W. D. *J. Biol. Chem.* **1954**, *207*, 341–351.

(20) Solomonson, L. P.; Lorimer, G. H.; Hall, R. L.; Borchers, R.; Bailey, J. L. *J. Biol. Chem.* **1975**, *250*, 4120–4127.

(21) Richardson, D. J.; Berks, B. C.; Russell, D. A.; Spiro, S.; Taylor, C. J. *Cell. Mol. Life Sci.* **2001**, *58*, 165–178.

(22) Bender, D.; Schwarz, G. *FEBS Lett.* **2018**, *592*, 2126–2139.

(23) Lundberg, J. O.; Weitzberg, E.; Gladwin, M. T. *Nat. Rev. Drug Discovery* **2008**, *7*, 156–167.

(24) Yang, J.; Giles, L. J.; Ruppelt, C.; Mendel, R. R.; Bittner, F.; Kirk, M. L. *J. Am. Chem. Soc.* **2015**, *137*, 5276–5279.

(25) Zhang, Z.; Naughton, D.; Winyard, P. G.; Benjamin, N.; Blake, D. R.; Symons, M. C. *Biochem. Biophys. Res. Commun.* **1998**, *249*, 767–772.

(26) Butler, C. S.; Seward, H. E.; Greenwood, C.; Thomson, A. J. *Biochemistry* **1997**, *36*, 16259–16266.

(27) Girsch, P.; Vries, S. de. *Biochim. Biophys. Acta, Bioenerg.* **1997**, *1318*, 202–216.

(28) Kumita, H.; Matsuura, K.; Hino, T.; Takahashi, S.; Hori, H.; Fukumori, Y.; Morishima, I.; Shiro, Y. *J. Biol. Chem.* **2004**, *279*, 55247–55254.

(29) Moënne-Loccoz, P. *Nat. Prod. Rep.* **2007**, *24*, 610–620.

(30) Moënne-Loccoz, P.; Vries, S. de. *J. Am. Chem. Soc.* **1998**, *120*, 5147–5152.

(31) Smith, P. A. S.; Hein, G. E. *J. Am. Chem. Soc.* **1960**, *82*, 5731–5740.

(32) Gorelsky, S. I.; Ghosh, S.; Solomon, E. I. *J. Am. Chem. Soc.* **2006**, *128*, 278–290.

(33) Malagó, A.; Bouraoui, F.; Grizzetti, B.; Roo, A. de. *J. Hydrol.: Reg. Stud.* **2019**, *22*, 100592.

(34) Velthof, G. L.; Lesschen, J. P.; Webb, J.; Pietrzak, S.; Miatkowski, Z.; Pinto, M.; Kros, J.; Oenema, O. *Sci. Total Environ.* **2014**, *468-469*, 1225–1233.

(35) Strebel, O.; Duynisveld, W.H.M.; Böttcher, J. *Agric. Ecosyst. Environ.* **1989**, *26*, 189–214.

(36) Kallis, G. *Water Policy* **2001**, *3*, 125–142.

(37) Goodchild, R. G. *Environ. Pollut.* **1998**, *102*, 737–740.

(38) Laue, W.; Thiemann, M.; Scheibler, E.; Wiegand, K. W. Nitrates and Nitrites. In *Ullmann's encyclopedia of industrial chemistry,* 1st ed.; Bohnet, M., Ed.; Wiley Interscience, 1999; p 65.

(39) Berg, J. M.; Holm, R. H. *J. Am. Chem. Soc.* **1985**, *107*, 925–932.

(40) Craig, J. A.; Holm, R. H. *J. Am. Chem. Soc.* **1989**, *111*, 2111–2115.

(41) Jiang, J.; Holm, R. H. *Inorg. Chem.* **2005**, *44*, 1068–1072.

(42) Lim, B. S.; Donahue, J. P.; Holm, R. H. *Inorg. Chem.* **2000**, *39*, 263–273.

(43) Lim, B. S.; Holm, R. H. *J. Am. Chem. Soc.* **2001**, *123*, 1920–1930.

(44) Majumdar, A.; Pal, K.; Sarkar, S. *Inorg. Chem.* **2008**, *47*, 3393–3401.

(45) Jiang, J.; Holm, R. H. *Inorg. Chem.* **2004**, *43*, 1302–1310.

(46) Sung, K.-M.; Holm, R. H. *Inorg. Chem.* **2000**, *39*, 1275–1281.

(47) *Progress in inorganic chemistry;* Lippard, S. J., Ed., 1st ed.; Progress in Inorganic Chemistry; Wiley: New York, N.Y.

(48) Cotton, F. A.; Wilkinson, G. *Advanced inorganic chemistry*, 5th ed.; A Wiley-Interscience publication; Wiley: New York, 1988.

(49) Beckman, J. S.; Koppenol, W. H. *Am. J. Physiol.* **1996**, *271*, C1424-37.

(50) Casella, L.; Carugo, O.; Gullotti, M.; Doldi, S.; Frassoni, M. *Inorg. Chem.* **1996**, *35*, 1101–1113.

(51) Kujime, M.; Fujii, H. *Angew. Chem. Int. Ed.* **2006**, *45*, 1089–1092.

(52) Merkle, A. C.; Lehnert, N. *Dalton Trans.* **2012**, *41*, 3355–3368.

(53) Nasri, H.; Wang, Y.; Hanh, H. B.; Scheidt, W. R. *J. Am. Chem. Soc.* **1991**, *113*, 717–719.

(54) Garner, C. D.; Hyde, M. R.; Mabbs, F. E.; Routletge, V. I. *Nature* **1974**, *252*, 579–580.

(55) Ju, T. d.; Woods, A. S.; Cotter, R. J.; Moënne-Loccoz, P.; Karlin, K. D. *Inorg. Chim. Acta* **2000**, *297*, 362–372.

(56) Lin, R.; Farmer, P. J. *J. Am. Chem. Soc.* **2001**, *123*, 1143–1150.

(57) Franz, K. J.; Lippard, S. J. *J. Am. Chem. Soc.* **1999**, *121*, 10504–10512.

(58) Paul, P. P.; Karlin, K. D. *J. Am. Chem. Soc.* **1991**, *113*, 6331–6332.

(59) Schneider, J. L.; Carrier, S. M.; Ruggiero, C. E.; Young, V. G.; Tolman, W. B. *J. Am. Chem. Soc.* **1998**, *120*, 11408–11418.

(60) Bar-Nahum, I.; Gupta, A. K.; Huber, S. M.; Ertem, M. Z.; Cramer, C. J.; Tolman, W. B. *J. Am. Chem. Soc.* **2009**, *131*, 2812–2814.

(61) Majouga, A. G.; Beloglazkina, E. K.; Moiseeva, A. A.; Shilova, O. V.; Manzheliy, E. A.; Lebedeva, M. A.; Davies, E. S.; Khlobystov, A. N.; Zyk, N. V. *Dalton Trans.* **2013**, *42*, 6290–6293.

(62) Esmieu, C.; Orio, M.; Torelli, S.; Le Pape, L.; Pécaut, J.; Lebrun, C.; Ménage, S. *Chem. Sci.* **2014**, *5*, 4774–4784.

(63) Zhang, Y.; Hurley, K. D.; Shapley, J. R. *Inorg. Chem.* **2011**, *50*, 1534–1543.

(64) Liu, J.; Wu, D.; Su, X.; Han, M.; Kimura, S. Y.; Gray, D. L.; Shapley, J. R.; Abu-Omar, M. M.; Werth, C. J.; Strathmann, T. J. *Inorg. Chem.* **2016**, *55*, 2597–2611.

(65) Schachner, J. A.; Terfassa, B.; Peschel, L. M.; Zwettler, N.; Belaj, F.; Cias, P.; Gescheidt, G.; Mösch-Zanetti, N. C. *Inorg. Chem.* **2014**, *53*, 12918–12928.

(66) Liu, J.; Su, X.; Han, M.; Wu, D.; Gray, D. L.; Shapley, J. R.; Werth, C. J.; Strathmann, T. J. *Inorg. Chem.* **2017**, *56*, 1757–1769.

(67) Schachner, J. A.; Berner, B.; Belaj, F.; Mösch-Zanetti, N. C. *Dalton Trans.* **2019**, *48*, 8106–8115.

(68) Ballhausen, C. J.; Gray, H. B. *Inorg. Chem.* **1962**, *1*, 111–122.

(69) Winkler, J. R.; Gray, H. B. Electronic Structures of Oxo-Metal Ions. In *Molecular electronic structures of transition metal complexes*; Mingos, D. M. P., Day, P., Dahl, J. P., Eds.; Structure and Bonding 142-143; Springer: Heidelberg, New York, 2012; pp 17–28.

(70) Espenson, J. H. *Coord. Chem. Rev.* **2005**, *249*, 329–341.

(71) Espenson, J. H.; Shan, X.; Wang, Y.; Huang, R.; Lahti, D. W.; Dixon, J.; Lente, G.; Ellern, A.; Guzei, I. A. *Inorg. Chem.* **2002**, *41*, 2583–2591.

(72) Wang, Y.; Espenson, J. H. *Inorg. Chem.* **2002**, *41*, 2266–2274.

(73) Arias, J.; Newlands, C. R.; Abu-Omar, M. M. *Inorg. Chem.* **2001**, *40*, 2185–2192.

(74) Brower, D. C.; Templeton, J. L.; Mingos, D. M. P. *J. Am. Chem. Soc.* **1987**, *109*, 5203–5208.

(75) Demachy, I.; Jean, Y. *Inorg. Chem.* **1997**, *36*, 5956–5958.

(76) Lippert, C. A.; Arnstein, S. A.; Sherrill, C. D.; Soper, J. D. *J. Am. Chem. Soc.* **2010**, *132*, 3879–3892.

(77) Wiedemaier, F. Theoretical Investigation of an Oxorhenium(V)-Complex catalysed Nitrate Reduction. Bachelor Thesis, Karl-Franzens Universität, Graz, 2018.

(78) Elgrishi, N.; Rountree, K. J.; McCarthy, B. D.; Rountree, E. S.; Eisenhart, T. T.; Dempsey, J. L. *J. Chem. Educ.* **2018**, *95*, 197–206.

(79) Fanwick, P. E.; Root, D. R.; Walton, R. A. *Inorg. Chem.* **1989**, *28*, 2239–2240.

(80) Travkin, V. F.; Antonov, A. v.; Kubasov, V. L.; Ishchenko, A. A.; Glubokov, Y. M. *Russ. J. Appl. Chem.* **2006**, *79*, 909–913.

(81) DuMez, D. D.; Mayer, J. M. *Inorg. Chem.* **1998**, *37*, 445–453.

(82) Elschenbroich, C. *Organometallchemie*, 5., überarb. Aufl.; Teubner-Studienbücher Chemie; Teubner: Wiesbaden, 2005.

(83) Rodrigues, V. H.; Costa, M. M. R. R.; Gomes, E. M.; Isakov, D.; Belsley, M. S. *Cent. Eur. J. Chem.* **2014**, *12*, 1016–1022.

(84) Yang, B.; Gagliardi, L.; Truhlar, D. G. *Phys. Chem. Chem. Phys.* **2018**, *20*, 4129–4136.

(85) Roy, K.-M. Sulfones and Sulfoxides. In *Ullmann's encyclopedia of industrial chemistry,* 1st ed.; Bohnet, M., Ed.; Wiley Interscience, 1999; p 157.

(86) Schachner, J. A., unpublished results.

(87) Tsukahara, H.; Ishida, T.; Mayumi, M. Gas-phase oxidation and disproportionation of nitric oxide. In *Nitric oxide detection, mitochondria and cell functions, and peroxynitrite reactions*; Cadenas, E., Packer, L., Eds.; Methods in Enzymology; Acad. Press: Amsterdam, 2002; pp 168–179.

(88) Eisenberg, R.; Meyer, C. d. *Acc. Chem. Res.* **1975**, *8*, 26–34.

(89) Ford, P. C.; Lorkovic, I. M. *Chem. Rev.* **2002**, *102*, 993–1018.

(90) Hayton, T. W.; Legzdins, P.; Sharp, W. B. *Chem. Rev.* **2002**, *102*, 935–992.

(91) Dziegielewski, J. O.; Machura, B.; Bartczak, T. J.; Czurak, W.; Kusz, J.; Warczewski, J. *J. Coord. Chem.* **1999**, *48*, 125–135.

(92) Abram, U.; Voigt, A.; Kirmse, R.; Ortner, K.; Hübener, R.; Carballo, R.; Vazquez-Lopez, E. *Z. Anorg. Allg. Chem.* **1998**, *624*, 1662–1668.

(93) Bartczak, T. J.; Czurak, W.; Dziegielewski, J. O.; Machura, B.; Jankowska, A.; Kusz, J.; Warczewski, J. *Polyhedron* **1999**, *18*, 2313–2320.

(94) Bartczak, T. J.; Czurak, W.; Dziegielewski, J. O.; Machura, B.; Jankowska, A.; Kusz, J.; Warczewski, J. *J. Coord. Chem.* **2001**, *52*, 361–373.

(95) Fujii, S.; Yoshimura, T. *Coord. Chem. Rev.* **2000**, *198*, 89–99.

(96) Vanin, A. F.; Liu, X.; Samouilov, A.; Stukan, R. A.; Zweier, J. L. *Biochim. Biophys. Acta, Gen. Subj.* **2000**, *1474*, 365–377.

(97) Chant, R.; Hendrickson, A. R.; Martin, R. L.; Rohde, N. M. *Inorg. Chem.* **1975**, *14*, 1894–1902.

(98) Maia, L. B.; Moura, J. J. G. *Methods Mol. Biol.* **2016**, *1424*, 81–102.

(99) Ophem, P. W.; Beeumen, J.; Duine, J. A. *Eur. J. Biochem.* **1993**, *212*, 819–826.

(100) Park, H.; Lee, H.; Ro, Y. T.; Kim, Y. M. *Microbiology* **2010**, *156*, 463–471.

(101) Kundu, S.; Stieber, S. C. E.; Ferrier, M. G.; Kozimor, S. A.; Bertke, J. A.; Warren, T. H. *Angew. Chem. Int. Ed.* **2016**, *55*, 10321–10325.

(102) Williams, K. d.; Cardenas, A. J. P.; Oliva, J. d.; Warren, T. H. *Eur. J. Inorg. Chem.* **2013**, *2013*, 3812–3816.

(103) Ridouane, F.; Sanchez, J.; Arzoumanian, H.; Pierrot, M. *Acta Crystallogr., Sect. C: Cryst. Struct. Commun.* **1990**, *46*, 1407–1410.

(104) Liebeskind, L. S.; Sharpless, K. B.; Wilson, R. d.; Ibers, J. A. *J. Am. Chem. Soc.* **1978**, *100*, 7061–7063.

(105) Leipoldt, J. G.; Coppens, P. *Inorg. Chem.* **1973**, *12*, 2269–2274.

Appendix

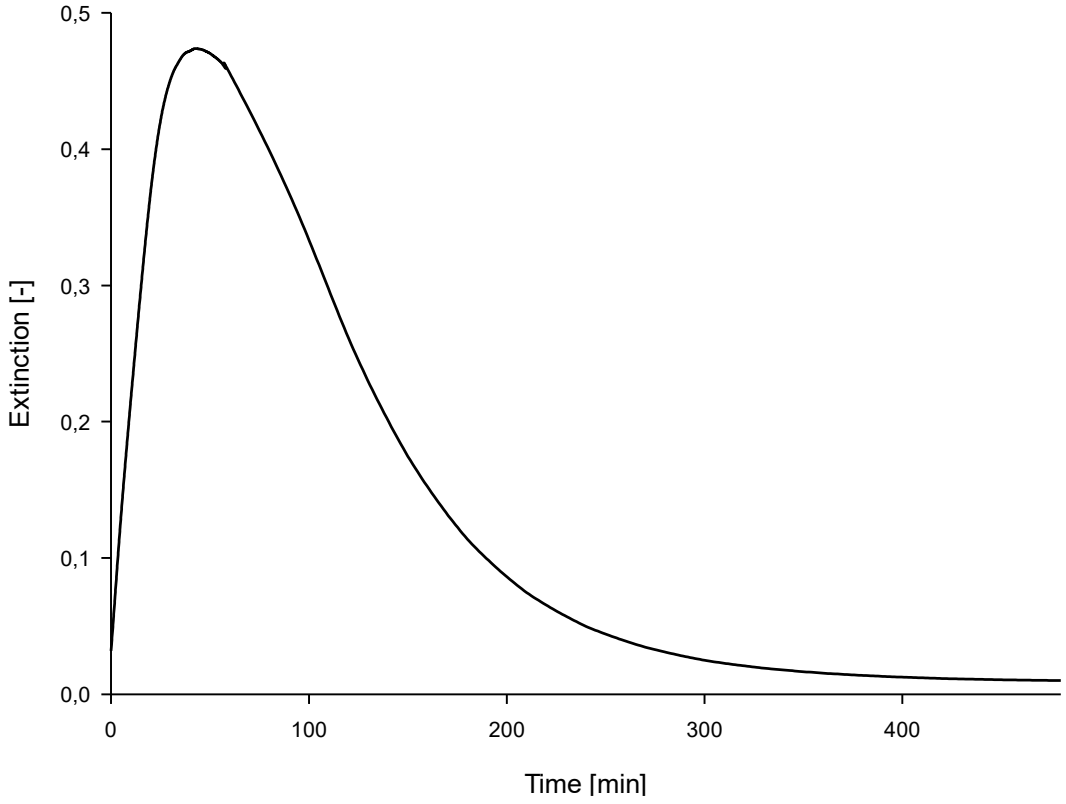

Figure 31 Progression of the extinction at 540 nm in a 1.7 µmol/L solution of **2** in acetonitrile after the addition of 10 equivalents $(Bu_4N)NO_3$ at room temperature

Table 3 Pseudo-first order rate constants at different temperatures of the formation (k'1) and the decay (k'2) of **3**; 20 µmol (100 equiv.) $(Bu_4N)NO_3$ were added to 2 ml of a tempered 0.1 mM solution of **2** in acetonitrile and the progression was measured at 540 nm; pseudo-first order rate constants were obtained by non-linear least squares fits

	20 °C	30 °C	40 °C	50 °C
k'_1 [10^{-5} s^{-1}]	22±1	54±1	137±9	276±2
k'_2 [10^{-5} s^{-1}]	5.7±0.4	15±1	41±1	97±3

Table 4 Raw-data of the kinetic investigations of the experiment described in Table 3

T [K]	k1' [s^{-1}]	k2' [s^{-1}]
323.14	0.0027418	0.0009435
323.14	0.0027685	0.0009577
323.14	0.0023310	0.0009948
313.14	0.0012703	0.0004015
313.14	0.0013878	0.0004062
313.14	0.0014430	0.0004238
303.14	0.0005327	0.0001390
303.14	0.0005275	0.0001508
303.14	0.0005495	0.0001627
293.14	0.0002085	0.0000573
293.14	0.0002307	0.0000600
293.14	0.0002217	0.0000530

Table 5 Progression of the reductive peak-current of the **3**/**3'** redox-couple (as in Figure 20) after the addition of 30 equivalent $(Bu_4N)NO_3$ to a 1.0 mM solution of **2** in dry acetonitrile containing 100 mg Bu_4NPF_6 as electrolyte; the upper values describe the formation of **3** during the reaction, the lower ones its decomposition

t [min]	I_{red} [µA]
formation	
13	20.2
15	21.9
19	24.4
20	25.1
23	26.8
decomposition	
60	27.3
80	23.8
100	20.1
120	16.5
140	14.6
170	10.1
225	5.8